UNIVERSITY OF CALIFORNIA SAN DIEGO

Function of the μ-opioid Receptor in Gonadotropin-releasing Hormone Neurons

A thesis submitted in partial satisfaction of the
requirements for the degree Master of Science

in

Biology

by

Laura Jane Cui

Committee in charge:

Pamela Mellon, Chair
Nicholas Spitzer, Co-chair
Stanley Lo

2019

The Thesis of Laura Jane Cui is approved, and it is acceptable in quality and form for publication on microfilm and electronically:

Co-chair

Chair

University of California San Diego

2019

DEDICATION

I'd like to dedicate my thesis to:

My parents and Rucy, for their love and support

Karen, Austin, Lukas, Teresa, Victoria, and Heejeong for the fun times in lab

My laundry girls, for our years of friendship and adventures

TABLE OF CONTENTS

LIST OF FIGURES AND TABLES

LIST OF ABBREVIATIONS

AC	Adenylyl Cyclase
ARC	Arcuate Nucleus
β-gal	Beta-galactosidase
cAMP	cyclic adenosine monophosphate
CRE	cAMP Response Element
CREB	cAMP Response Element Binding Protein
CRE-luc	pGL3 – minTK – CRE – luc
Derm A584	Dermorphin-Alexa594
DMSO	dimethyl sulfoxide
E_2	Estrogen
FSH	Follicle-Stimulating Hormone
FSK	Forskolin
GIRK	G-protein Gated Inwardly Rectifying Potassium
GnRH	Gonadotropin-releasing Hormone
GPCR	G-protein Coupled Receptor
HPG	Hypothalamic Pituitary Gonadal
Kiss1	Kisspeptin
KO	Knockout
LH	Luteinizing hormone
μOR	μ-Opioid Receptor
OIH	Opioid-Induced Hypogonadism

ORL	Opioid Receptor Like
Oprm1	pcDNA3.1 - μOR vector
Oprm1	gene for the μOR
POA	Preoptic Area
PKA	Protein Kinase A
T	Testosterone
WT	Wildtype

ACKNOWLEDGEMENTS

I would like to acknowledge my post-doctoral fellow mentor, Dr. Karen Tonsfeldt, and the chair of my committee, Dr. Pamela Mellon, for their patience, support, and guidance over these last 3 years. Their help has shaped me into the scientist I am today, and I am incredibly grateful for their mentorship.

I would also like to acknowledge my committee members, Dr. Stanley Lo and Dr. Nicholas Spitzer, for their support and interest in my work.

Finally, I would like to thank the members of the Mellon lab for creating such a supportive community.

ABSTRACT OF THE THESIS

Function of the μ-opioid Receptor in Gonadotropin-releasing Hormone Neurons

by

Laura Jane Cui

Master of Science in Biology

University of California San Diego, 2019

Professor Pamela L. Mellon, Chair
Professor Nicholas Spitzer, Co-chair

With the emergence of wide-spread opioid use, it is becoming increasingly important to understand the non-analgesic effects of opioids. One such side effect is the decrease in sex steroid production, a phenomenon called opioid-induced hypogonadism (abbreviated here OIH). OIH can occur in both males and females and is thought to develop through opioid suppression of the hypothalamic-pituitary-gonadal (HPG) axis. OIH is characterized by the suppression in

estrogen (E_2) and testosterone (T) that arises after acute or chronic opioid exposure. Previous studies have shown the hypothalamus to be the main target of opioid action; however, the exact mechanism is still unknown. This thesis aims to illustrate the function of the μ-opioid receptor (μOR) in gonadotropin-releasing hormone neurons of the hypothalamus and how that may relate to the development of OIH.

We have found that immortalized GnRH neurons (GT1-7 cells) express function μOR, allowing us to use GT1-7 cells as the ideal *in vitro* model to test for cellular changes in GnRH neurons after opioid exposure. Using a cAMP Response Element luciferase (CRE-luc) reporter vector to measure transcription, we were able to illustrate that isoproterenol (ISO) and forskolin (FSK) activate CRE-luc in a dose-dependent manner. After morphine cotreatment, we saw an attenuation of ISO-induced CRE-luc activation, indicating opioid suppression of this pathway. We did not see any change in the FSK-induced CRE-luc activation after morphine cotreatment. However, overexpression of the μOR caused an enhanced inhibition of CRE-luc activation in both ISO and FSK cotreated cells. These findings suggest that μOR signals through a Gi pathway in immortalized GnRH neurons, and may alter GnRH neuron transcription by attenuating CRE-mediated transcription. In addition, we found that morphine pretreatment *in vivo* alters GnRH neuron responsiveness to the hormone kisspeptin, as measured via luteinizing hormone (LH) output. Morphine pretreatment does not change pituitary responsiveness to GnRH, indicating a hypothalamic role of morphine. In mutant mice where μOR is selectively deleted from GnRH neurons, morphine pretreatment is unable to suppress kisspeptin activation of GnRH neurons. These results suggest that μOR activation in GnRH neurons is needed for morphine-mediated suppression of the HPG axis. Unexpectedly, chronic morphine treatment in female mice did not significantly alter gene expression in the hypothalamus, pituitary, or ovaries.

These findings illustrate that chronic morphine use may not permanently alter expression of key reproductive genes. Overall, these findings suggest that opioid action via the μOR in GnRH neurons plays a key role in the suppression of the HPG axis. Future studies must be conducted to fully define altered GnRH activity and secretion in the development of OIH.

INTRODUCTION

In 2015, the National Survey on Drug Use and Health (NSDUH) reported that a third of Americans use prescription opioids (1). Opioids are commonly used for pain relief, but there are numerous off target effects. One side effect that affects both males and females is hypogonadism (2). Hypogonadism is a general condition characterized as a decrease in sex steroids, and sex steroid reduction due to opioid use is called opioid-induced hypogonadism (abbreviated here as OIH) (3, 4). The sex steroids, testosterone (T) and estrogen (E_2), are important for regulating numerous physiological systems, and hypogonadism leads to suppression of those systems (5). For example, people diagnosed with hypogonadism suffer from sexual dysfunction, early onset of osteoporosis, lower quality of life, absent puberty, and abnormal fertility (2, 4). Fertility and the sex steroids are regulated by the brain through the hypothalamic-pituitary-gonadal (HPG) axis. Opioids drive hypogonadism by inhibition of the HPG axis (6); however, not much is known about the mechanisms that drive the development of OIH.

The central reproductive axis – The HPG axis

The HPG axis is composed of three main sites: the hypothalamus, the pituitary gland, and the gonads. The hypothalamus is composed of bundles of nuclei in the brain that regulate numerous homeostatic centers, such as the pituitary (7). The anterior pituitary regulates peripheral endocrine organs, such as the gonads (8). The gonads, ovaries for females and testes for males, are responsible for regulating reproductive function. For males and females, the HPG axis comprises of Kiss1 neurons in the arcuate nucleus (ARC) of the hypothalamus that secrete the neuropeptide kisspeptin onto gonadotropin-releasing hormone (GnRH) neurons in the preoptic area (POA) of the hypothalamus (9) (**Figure 1**). Kisspeptin stimulation prompts GnRH

neurons to secrete the neuropeptide GnRH in a pulsatile manner onto the anterior pituitary (9) (**Figure 1**). This stimulates the anterior pituitary to secrete the gonadotropins luteinizing hormone (LH) and follicle-stimulating hormone (FSH) into the bloodstream to act on the gonads (9) (**Figure 1**). LH and FSH stimulate the gonads to grow and secrete T or E_2, which negatively feedback on the hypothalamus and the pituitary to homeostatically regulate sex steroid concentrations (10) (**Figure 1**). In females, E_2 can positively feedback back on a second population of Kiss1 neurons in the anteroventral periventricular nucleus (AVPV) of the hypothalamus to drive the preovulatory LH surge that causes ovulation (**Figure 1**)**.** In OIH, downstream effects of opioid action cause the gonads to secrete reduced amounts of sex steroids.

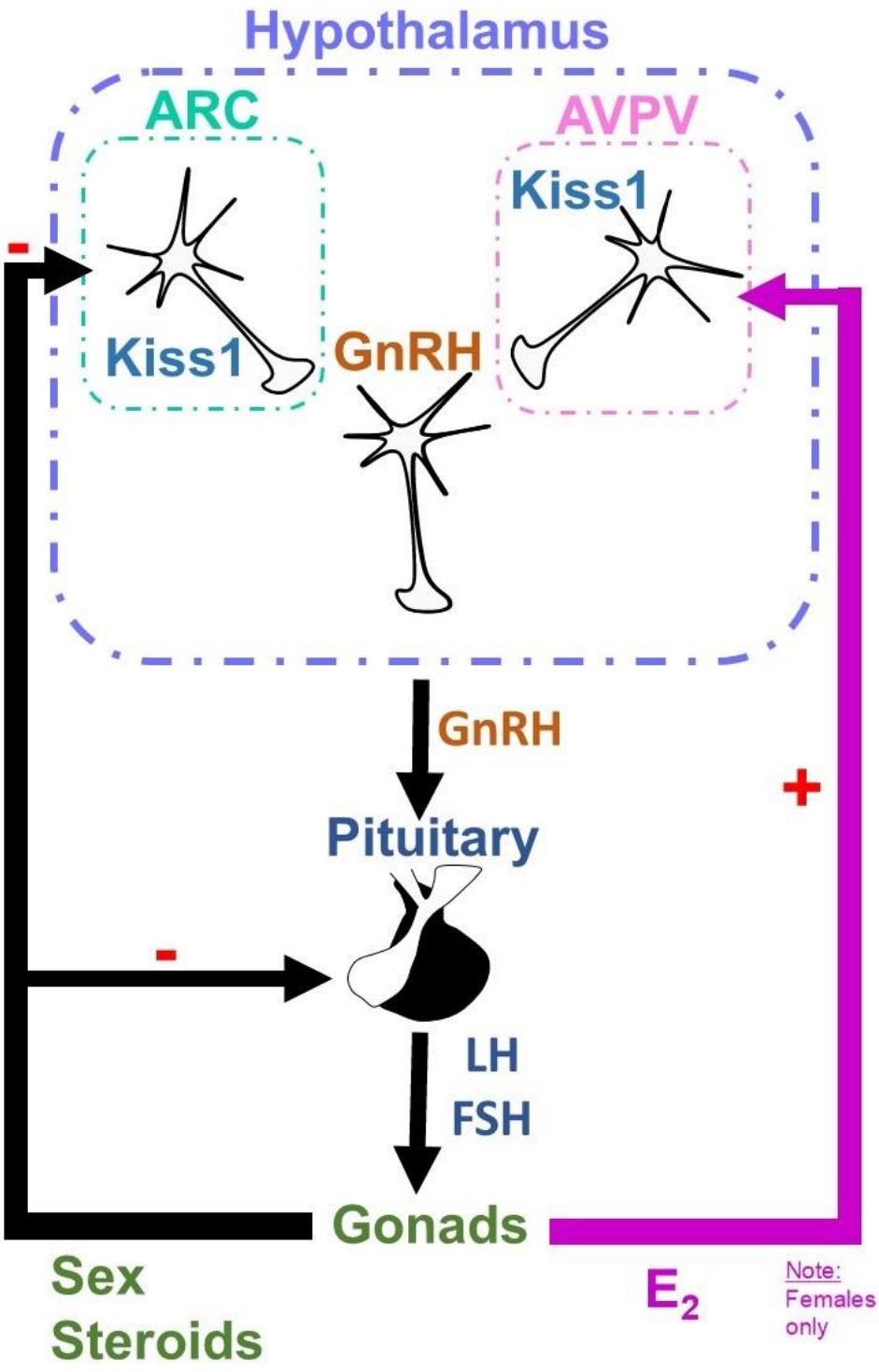

Figure 1: **The HPG axis regulates reproductive function.** ARC Kiss1 neurons in the hypothalamus secrete the neuropeptide kisspeptin onto GnRH neurons. This stimulates the GnRH neurons to secrete the neuropeptide GnRH onto the anterior pituitary, resulting in LH and FSH secretion to act on the gonads. Consequently, the gonads secrete the sex steroids to negatively feedback at the pituitary and the hypothalamus. In females, high E_2 results in positive feedback on AVPV Kiss1 neurons to induce the preovulatory surge.

Opioid action on the HPG axis - the μ-opioid receptor

Opioid action on the hypothalamus can cause the downstream decrease in sex steroid secretion. Previous studies have shown that opioids cause a decrease in GnRH neuronal activity (11). Opioids have been shown to reduce overall LH secretion, which drives the decreased sex steroid secretion from the gonads that results in hypogonadism (11). When the connection between the hypothalamus and the pituitary is lesioned in rats, morphine treatment does not alter serum LH (12). This indicates the hypothalamus to be the main site of opioid action, but the exact mechanism of OIH is still unclear. Opioid action on any site of the HPG axis could drive the downstream effects of decreased LH and sex steroid production.

At a cellular level, opioids bind to four main classes of opioid receptors: the μ class, the κ class, the δ class, and the opioid-receptor-like (ORL) class (13). Previous studies show that selective μ-opioid receptor (μOR) agonists cause decreased LH secretion and GnRH hyperpolarization (14, 15, 16), indicating that OIH most likely arises due to μOR activation. μOR activation has been studied in various cell types (13); however, the μOR has not been directly studied in the relevant sites of the HPG axis. The μOR is an inhibitory G-protein coupled receptor (GPCR), and μOR activation can cause numerous inhibitory effects (13).

Cellular mechanism of μOR activation

When activated, the α_i and βγ subunits of the μOR dissociate from the membrane. The βγ subunit inhibits Ca^{2+} influx through N-type calcium channels while the α_i subunit activates G-protein gated inwardly rectifying potassium channels (GIRK) and inhibits adenylyl cyclase (AC) (13, 17) (**Figure 2**). Inhibition of Ca^{2+} channels attenuates depolarization and vesicle release,

affecting peptide secretion. Activation of GIRK channels promotes K^+ efflux, effectively decreasing cellular potential and inhibiting cellular activation. Inhibition of AC results in decreased cyclic AMP (cAMP) synthesis, decreasing cAMP cellular concentrations (13) (**Figure 2**). Reduction in cAMP concentrations leads to a suppression of cAMP-mediated signaling pathways. For example, cAMP activates protein kinase A (PKA), which can phosphorylate transcription factors such as cAMP response element binding protein (CREB) (18) (**Figure 3**). Phosphorylated CREB will dimerize and directly bind to cAMP response element (CRE) sites in promoter regions, which lead to changes in gene expression (18) (**Figure 3**). Reduction in cAMP will suppress PKA activity, therefore altering CREB activation and CRE-mediated transcription.

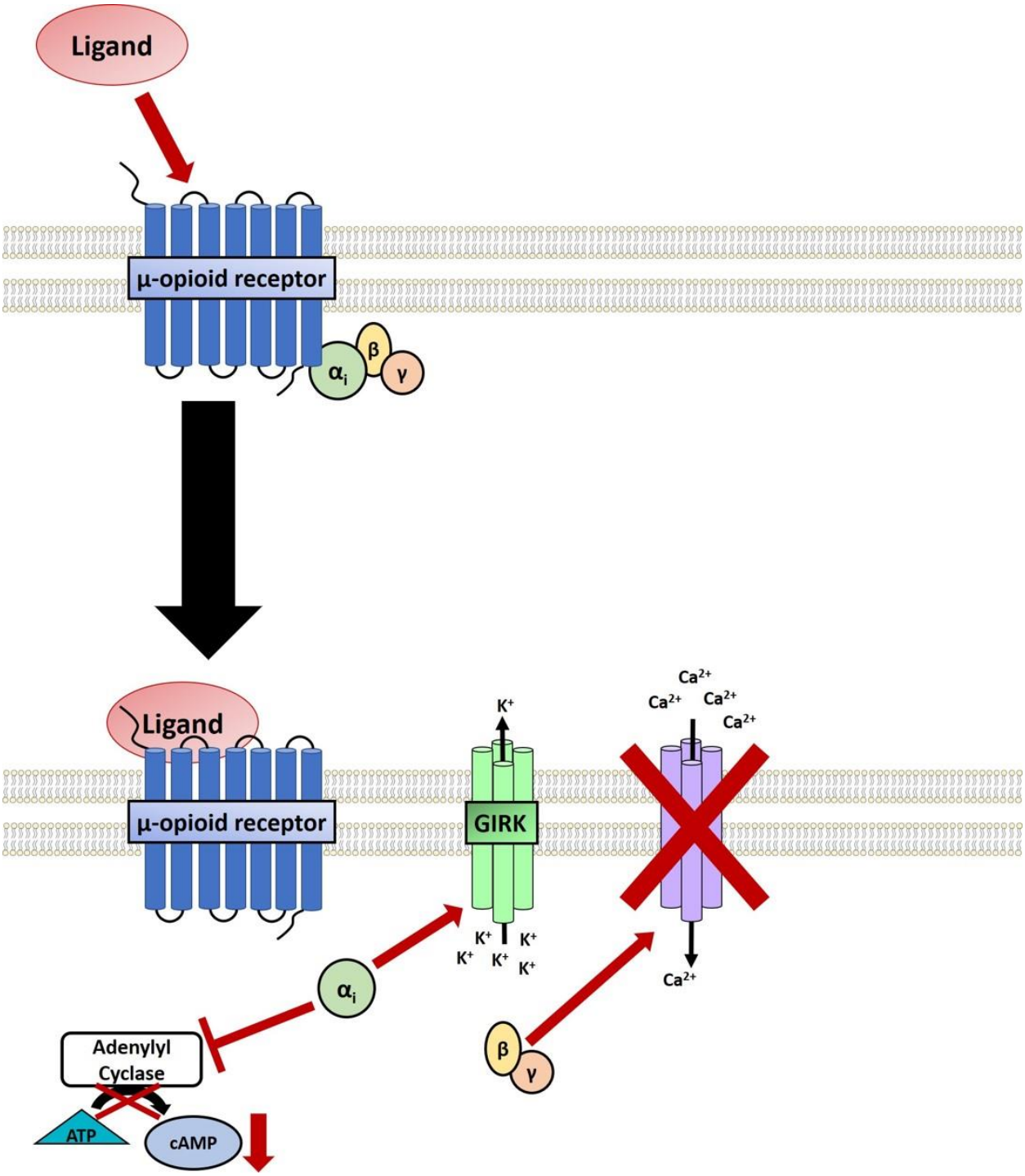

Figure 2: Characteristics of acute μOR activation. Acute activation of the μOR causes the α_i subunit to dissociate and inhibit adenylyl cyclase. This inhibition decreases the cAMP synthesis. The α_i subunit also activates GIRK channels, causing inhibition of cellular activity. The dissociation of the βγ subunits inhibits Ca^{2+} influx, subsequently decreasing cellular activity and secretion.

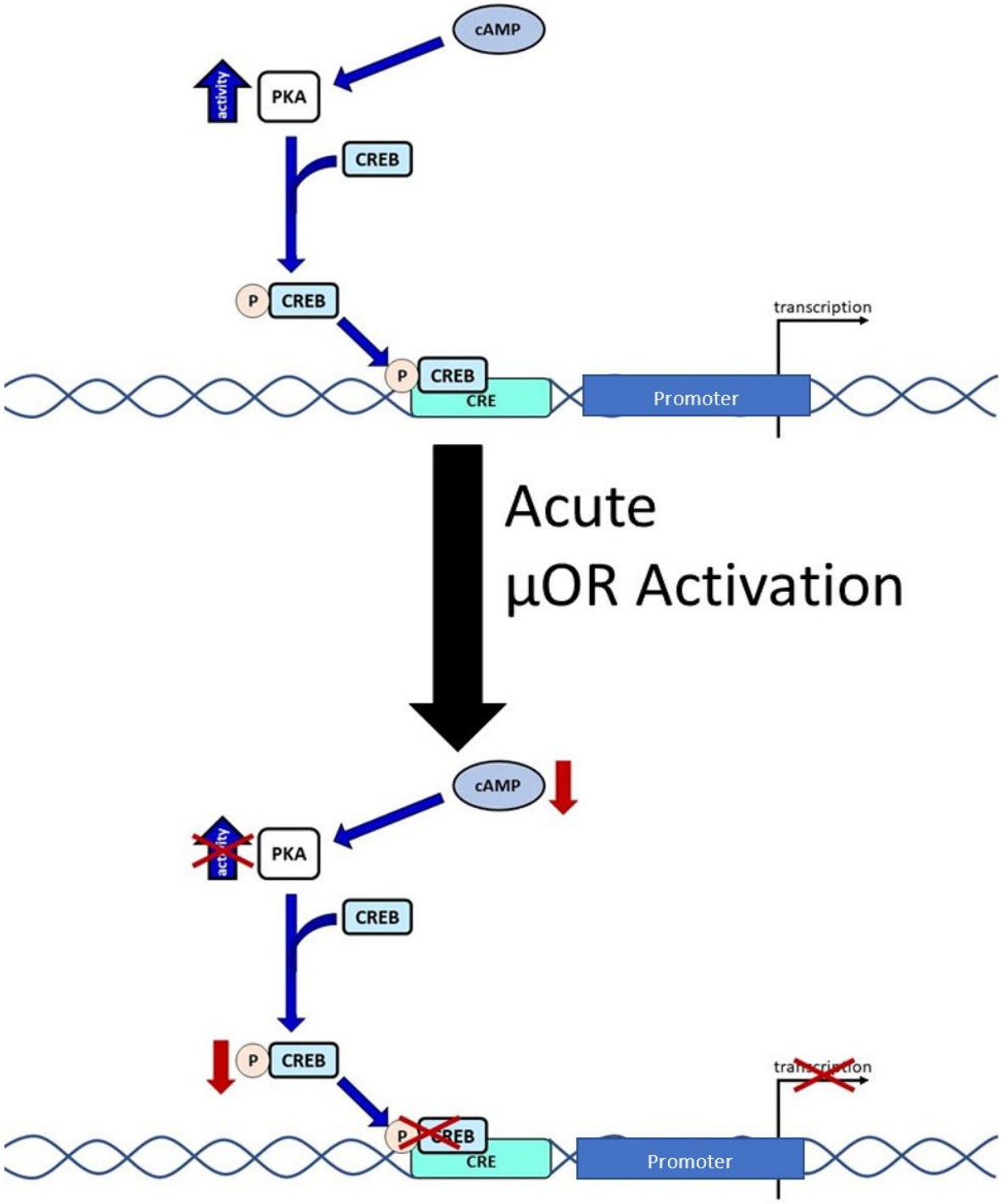

Figure 3: cAMP signaling pathway and μOR effects on cAMP signaling. cAMP directly binds and activates PKA. PKA will phosphorylate the transcription factor CREB, which allows it to bind to the CRE region of a promoter and alter transcription. Acute μOR activation leads to a decrease in cAMP, which will lead to a decrease in PKA activity. This decreased PKA activity will decrease the amount of phosphorylated CREB, and consequently decrease CRE-mediated transcription.

Hypothesis

Increased use of opioids has made it increasingly important to understand the mechanism behind OIH. This project aims to establish the role of μOR in GnRH neurons, and how this might contribute to the development of OIH. We hypothesize that μOR is functional in GnRH neurons, signals through Gi, and inhibits GnRH neuron function.

MATERIALS AND METHODS

Cell culture

Immortalized GT1-7 cells were derived from mouse hypothalamic GnRH neurons (19). Cells were maintained in DMEM (Mediatech, Manassas VA) with 10% fetal bovine serum (Omega, Tarzana CA) and 1% penicillin/streptomycin (HyClone, Pittsburgh PA). Cells were incubated at 37ºC with 5% CO_2. Cells passaged between 14 and 30 were used for experiments.

Plasmid Constructs

CRE-mediated transcription was measured by creating a luciferase reporter plasmid construct. The plasmid was created using a pGL3-luciferase reporter vector containing a minimal thymidine kinase promoter (135 bp) (pGL3-minTK-luc) located -138 to -50 from the transcription start site. A CRE oligonucleotide (87 bp) was ordered (IDT, San Diego CA) and inserted into the pGL3–minTK–luc at the XhoI and NheI restriction sites (-235 to -138 from the transcription start site), creating a CRE-luc (pGL3–minTK–CRE–luc). The pGL3–minTK–luc empty vector was used as a control. A μOR overexpression vector was created using a pcDNA3.1 luciferase reporter vector containing the μOR gene (*Oprm1*) (20). All plasmids were grown in DH5α competent cells (Invitrogen, Carlsbad CA). Plasmids were extracted using a DNA Maxiprep Kit (Qiagen, Venlo Netherlands) and then sequenced by Eton Biosciences (San Diego, CA) to confirm the presence of desired sequences. A vector expressing *β-galactosidase* (β-gal) downstream of the thymidine kinase promoter was used to normalize luciferase values.

Luciferase reporter assay

Assays began with seeding GT1-7 cells at a density of 250,000 cells per mL in 12-well plates. 24 hours after seeding, cells were transfected with the PolyJet reagent (SignaGen) at a 3:1

ratio of PolyJet to DNA. For each experiment, GT1-7 cells were transfected with 50 ng of β-gal per well. Cells were transfected with 200 ng of CRE-luc or 200 ng of empty vector pGL3–minTK–luc. In the overexpression experiment, cells were co-transfected with 200 ng Oprm1 or 200 ng of empty vector pcDNA3.1 along with the CRE-luc or respective empty vector. About 6 hours after the PolyJet-plasmid DNA mixture was added, media was changed. One day later, cells were treated for 6 hours. After treatment, media was aspirated, and cells were washed in PBS (Mediatech). Cells were harvested by adding 60 µL of a lysis solution (91.5 mM K_2HPO_4, 8.5 mM KH_2PO_4, 0.2% Triton X-100), and 25 µL of lysed cells were used to measure luciferase and β-gal. Luciferase was measured by adding 100 µL of a luciferase assay buffer (25mM Tris pH 7.4, 15mM $MgSO_4$, 250 mM ATP, 65 µM firefly D-luciferin Fisher Scientific) to the lysed cells. Luminescence was measured 1 second after the addition of the buffer. β-gal was measured 1 second after 100 µL of Tropix Accelerator II was added to a mixture of lysed cells and Galacton Reagent (99% Tropix Galacton Diluent, 1% Tropix Galacton Plus). All luminescence measurements originated from a Veritas Microplate luminometer (Turner Biosystems).

Luciferase Data Analysis

Background activity was recorded and averaged. The averaged background values were subtracted from all luciferase and β-gal values. Luciferase values were divided by β-gal values to normalize for transfection efficiency. The respective empty vector luciferase/β-gal values were averaged, and the CRE-luc luciferase values were divided by the respective empty vector averages. For example, the 100 nM ISO treated CRE-luc cells were divided by the average of the 100 nM ISO treated pGL3–minTK–luc cells. The luciferase values of cells co-transfected with the CRE-luc/pcDNA3.1 empty vector were divided by average luciferase values of cells co-transfected with pGL3–minTK–luc empty vector/ pcDNA3.1 empty vector. The luciferase values

of cells co-transfected with the CRE-luc/Oprm1 were divided by average luciferase values of cells co-transfected with pGL3–minTK–luc empty vector/Oprm1. Vehicle treated cell luciferase values were averaged, and all luciferase values were divided by the respective vehicle treated cells. Data were analyzed using a two-way ANOVA or Dunnett's multiple comparisons test in Graphpad (Prism), and significance was established with $p < 0.05$. All luciferase experiments were done in triplicate. Figures show averages and standard error of the mean (SEM) as error bars of the nine samples (N = 3).

Treatments

Cells were treated with 1 µM Dermorphin-A594 (DermA594) for 20 minutes. DermA54 was kindly provided by Dr. John Williams and Seksiri Arttamangkul. Isoproterenol (Tocris, Minneapolis MN) was dissolved in glass distilled water to create a 100 mM stock, which was stored at -20ºC until needed. For the ISO dose response curve (**Figure 6**), ISO was thawed the day of treatment, and pipetted into complete media to create 10 nM, 30 nM, 100 nM, 300 nM, and 1 µM ISO concentrations. Media was aspirated and replaced with a treatment-media mixture. The treatment-media mixture was left on cells for 6 hours before cells were harvested. Morphine (Sigma) was dissolved in water to create a 10 mM stock, which was stored at -20ºC. ISO-morphine co-treatment (**Figure 7**) was left on GT1-7 cells for 6 hours before harvest. Forskolin (FSK) (Abcam) was dissolved in dimethylsulfoxide (DMSO) to create a 10 mM stock and stored at -20ºC until needed. For the FSK dose response curve (**Figure 9**), FSK was thawed the day of treatment, and pipetted into complete media to create 100 nM, 300 nM, 1 µM, 3 µM, and 10 µM FSK concentrations. Transfected cells were treated with FSK for 6 hours and then harvested for luciferase. FSK-morphine co-treatment (**Figure 10**) was left on cells for 6 hours and then harvested.

Mice

All animal experiments were approved by the University of California, San Diego Institution Animal Care and Use Committee. Wildtype (WT) mice (C57BL/6J) were obtained from Jackson Laboratories (Bar Harbor ME). Conditional knock out *Oprm1* GnRH knockout (KO) mice were created by crossing an *Oprm1*$^{flox/flox}$ mouse (21) with a LHRH-Cre mouse (22). Exons 2 and 3 of the *Oprm1* gene were floxed in the *Oprm1*$^{f/f}$ mouse. All mice were housed at LD 12:12.

Hormone assays

Female mice were staged through vaginal cytology, and only females in diestrus were used for all the following experiments. For the LH pulse experiment (**Figure 12**), females were weighed and given 20 mg of morphine/kg of mouse or saline. Blood was collected via tail bleeds every 6 minutes for 60 minutes. For the GnRH hormone challenge (**Figure 13**), females were weighed and pretreated with 20 mg of morphine/kg of mouse or saline. Blood was collected 15 minutes later via tail bleeds, and all mice were injected intraperitoneally with 2 mg of GnRH/kg of mouse or saline. Post GnRH blood was collected 15 minutes later, 30 minutes after morphine treatment. For the Kiss1 hormone challenge (**Figure 14**), WT and *Oprm1* GnRH KO females were weighed and sorted into treatment groups. WT and *Oprm1* GnRH KO females were pretreated with saline or 20 mg of morphine/kg of mouse. Blood was collected 15 minutes later via tail bleed, and synthetic kisspeptin, called Kiss-10, was injected intraperitoneally. Post Kiss-10 blood was collected 15 minutes later.

Serum analysis

All blood samples were incubated at room temperature for 20 minutes to allow for blood clotting, then spun down at 2,000 *x* g for 15 minutes. Serum was pipetting into new tubes and kept in -20ºC until multiplex assay was conducted. Serum was added to matrix buffer from the Milliplex MAP mouse pituitary magnetic bead panel, and multiplex assays were conducted using Luminex Magpix to measure LH concentrations in serum samples.

Chronic morphine treatment

WT female mice were injected intraperitoneally twice a day for 7 days. Injections occurred 12 hours apart each day. The following concentrations were given per day: Day 1 - 20 mg of morphine/kg of mouse; Day 2 – 40 mg of morphine / kg of mouse; Day 3 – 60 mg of morphine / kg of mouse; Day 4 – 80 mg of morphine / kg of mouse; Day 5 – 100 mg of morphine / kg of mouse; Day 6 – 100 mg of morphine / kg of mouse; Day 7 – 100 mg of morphine / kg of mouse. On day 7, mice were sacrificed 4 hours after the first injection.

RNA isolation and cDNA synthesis

Tissue was collected at the time of sacrifice and placed in a 1:1 dilution of RNAlater reagent (Qiagen) and water. RNA was isolated according to the Qiagen protocol. RNA concentration was measured using a nanodrop, and all samples were diluted to 50 ng/µL (hypothalamus and ovary) or 100 ng/µL (pituitary). cDNA was made using the iScript gDNA Clear cDNA Synthesis Kit (Bio-rad, Hercules CA). cDNA was diluted to 1:5 for quantitative PCR (qPCR) analysis.

Quantitative PCR

Every qPCR reaction was made of 8 µL of master mix and 2 µL of diluted cDNA. Master mix for qPCR was made using 2.4 µL water, 0.3 µL of forward primer, 0.3 µL of reverse primer, and 5 µL of iQ SYBR Master Mix (Bio-rad). Reactions were run at an annealing temperature of 60ºC. The primer sequences are listed in **Table 1**.

qPCR analysis

All qPCR reactions were run in triplicate, and those triplicates were averaged. Standard deviations were taken, and any samples with a standard deviation greater than 0.5 were analyzed for outliers. Outliers were determined by the difference between the triplicates, where the difference between the middle value and the outlier values were calculated. The smallest difference was multiplied by 2 and compared to the largest difference. If the largest difference were smaller, then the value would be excluded by the analysis and the average Cq would be adjusted.

The housekeeping genes *H2afz* and *Ppia* were used for Cq normalization. The average of the *H2afz* and *Ppia* Cqs were averaged, and the average Cq of the genes of interest were subtracted by Cqs of the averaged housekeeping genes to give ΔCt. The ΔCt from control animals were averaged, and subtracted from the ΔCt of the genes of interest. This gives the ΔΔCt value. Average fold change of gene expression was calculated as $2^{-\Delta\Delta Ct}$. All primer sequences are listed in Table 1.

Table 1: Primer sequences used for qPCR. Both forward and reverse primers were used in qPCR.

Gene	Forward Primer (5' to 3')	Reverse Primer (5' to 3')
H2afz	TCACCGCAGAGGTACTTGAG	GATGTGTGGGATGACACCA
Ppia	AAGTTCCAAAGACAGCAGAAAAC	CTCAAATTTCTCTCCGTAGATGG
GPR54	GCACATGCAGACAGTTACC	GCAGCACAGTAGGAAAGTGAC
FSHβ	GCCGTTTCTGCATAAGC	CAATCTTACGGTCTCGTATACC
LHβ	CTGTCAACGCAACTCTGG	ACAGGAGGCAAAGCAGC
GnRH	CTACTGCTGACTGTGTGTTTG	CATCTTCTTCTGCCTGGCTTC
Oprm1	CCAGGGAACATCAGCGACTG	GTTGCCATCAACGTGGGAC
FSH-R	CTGGAGCAGGCAGAAAGCAG	CAGTTCAATGGCGTTCCG
LH-R	GGTTGTCAAAGGCATTAGCTTC	CCGACTATCTCTCACCTATCTCC
Cyp19a1	GAGTCTGGATCAGTGGAGAG	CACGCTTGCTGCCGAATC
STAR	CAGGAAGAACAACCCTTGAGC	GAACTTGACCCATCCACC
AMH	TCCAGGGTATAGCACTAACAGG	GTCCTACATCTGGCTGAAGTG

RESULTS

CHAPTER I: Morphine treatment alters CRE-mediated transcription through μ-opioid receptor activation

Previous studies have established that OIH most likely arises due to μ-opioid receptor (μOR) activation (14, 15, 16). Since the μOR is an inhibitory GPCR, we hypothesized activation of the μOR in GnRH neurons would decrease cAMP synthesis. A reduction in cAMP would result in reduced CRE-mediated transcription, altering gene expression in GnRH neurons.

Immortalized GnRH neurons (GT1-7) express functional μ-opioid receptor (μOR)

This first experiment was conducted to establish the presence of functional μOR in the immortalized GnRH neurons (GT1-7). The GT1-7 cells were treated with a fluorescently conjugated μOR agonist called Dermorphin-Alexa594 (Derm A584). After 20 minutes, the cells were placed under a microscope to visualize receptor binding and internalization. The distinct red fluorescence inside the illustrated GT1-7 cell indicates μOR internalization, which marks the presence of functional μOR (**Figure 4**). This illustrates that the GT1-7 cells can responsive to opioid treatment.

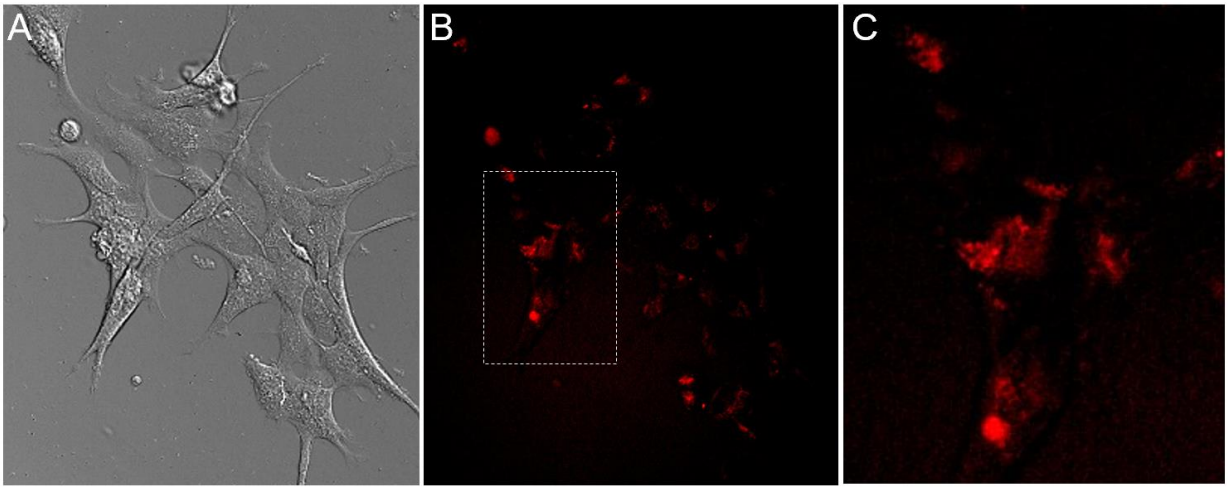

Figure 4: GT1-7 cells express functional μOR. Panel A shows multiple GT1-7 cells before Derm A584 exposure. Panel B shows the GT1-7 cells after Derm A584 exposure, where the Derm A584 was bound to μOR and internalized. Panel C is a close-up of one GT1-7 cell, indicated by the box in Panel B, where internalization of the fluorescent Derm A584 is clearly indicated.

.

Isoproterenol induces CRE-luc activity

Since the μOR activation inhibits AC activity to decrease cAMP synthesis (13), we wanted to examine if we could measure transcriptional changes due to altered cAMP concentrations. Increased cAMP concentrations have been known to increase PKA activity, therefore increasing CREB phosphorylation and CRE-mediated transcription (23) . We created a CRE luciferase (CRE-luc) reporter vector as a way to measure cAMP via CRE-mediated transcription (**Figure 5**). We transfected the GT1-7 cells with the CRE-luc and treated the cells with isoproterenol (ISO), a known β-adrenergic receptor agonist that activates cAMP synthesis, for 6 hours. As the concentrations of ISO treatments increased, CRE-luc activity also increased (10 nM ISO: 1.58 ± 0.19; 30 nM ISO: 1.55 ± 0.35; 100 nM ISO: 3.33 ± 0.81; 300 nM ISO: 3.09 ± 0.35; 1 μM ISO: 4.06± 0.37) (**Figure 6**). This illustrates that ISO induces changes in CRE-luc activity in a dose-dependent manner, likely through increased cAMP concentrations.

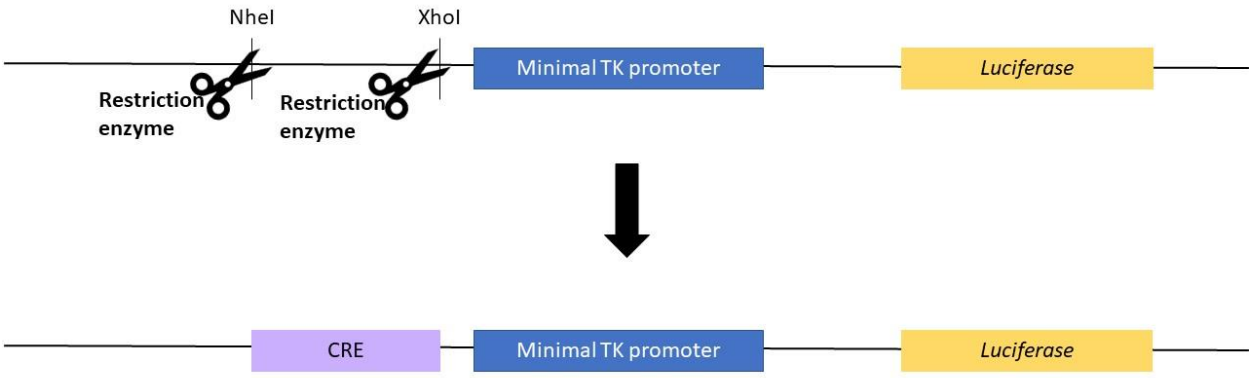

Figure 5: CRE-luc plasmid construct. A CRE sequence was ligated upstream of a minimal TK promoter. Downstream of the promoter is a *Luciferase* gene used to measure transcription.

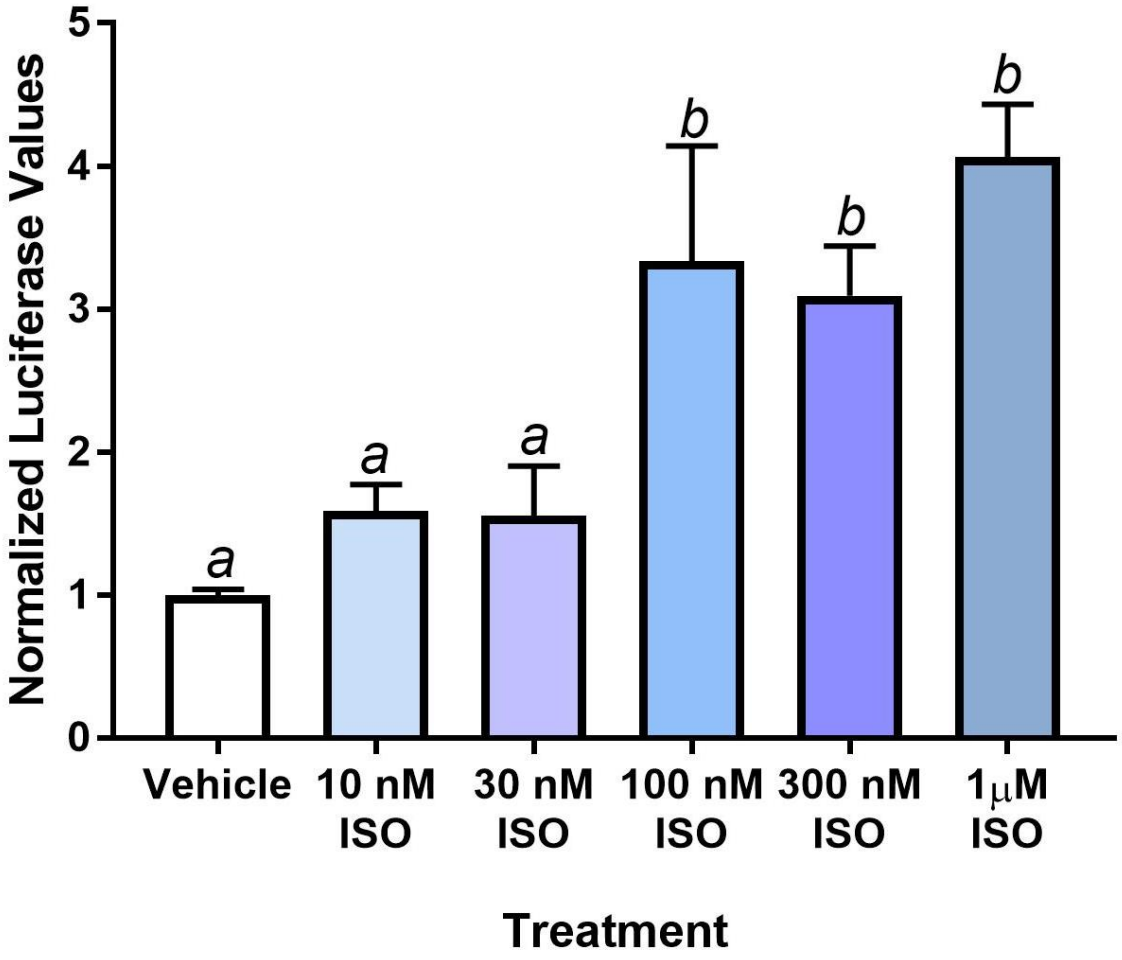

Figure 6: Isoproterenol (ISO) induces CRE-luc expression in a dose-dependent manner. GT1-7 cells were transfected with CRE-luc and treated with ISO for 6 hours. Normalized CRE-luc expression increases in a dose-dependent manner. N = 3 and error bars indicate standard error of the mean (SEM). Data were analyzed with one-way ANOVA and Dunnett's multiple comparison test, where "*b*" denotes $p < 0.05$ compared to vehicle treatment.

Morphine can attenuate the ISO-induced CRE-luc activation

Next, we wanted to see if morphine treatment could alter ISO-induced CRE-luc activation. Morphine, a commonly used opioid, binds to the μOR to inhibit adenylyl cyclase and decreases cAMP synthesis (13). We chose 100 nM ISO as the optimal concentration (giving a luciferase average of 3.99 ± 0.53), and co-treated the transfected cells with morphine for 6 hours (100 nM ISO + 10 nM morphine: 3.28 ± 0.53; 100 nM ISO + 100 nM morphine: 3.77 ± 0.51; 100 nM ISO + 1 μM morphine: 2.45 ± 0.25) (**Figure 7**). Dunnett's multiple comparisons test was conducted to compare luciferase averaged values to those of the different treatment groups (vehicle vs. 100 nM ISO: $p<0.0001$; vehicle vs. 100 nM ISO and 10 nM morphine: $p = 0.0021$; vehicle vs. 100 nM ISO and 100 nM morphine: $p = 0.0002$; vehicle vs. 100 nM ISO and 1 μM morphine: $p = 0.06$) (**Figure 7**). There was no significant difference found between the vehicle treated GT1-7 cells and the 100 nM + 1 μM morphine co-treated cells, indicating an attenuation of the ISO-induced CRE-luc activity by morphine (**Figure 7**).

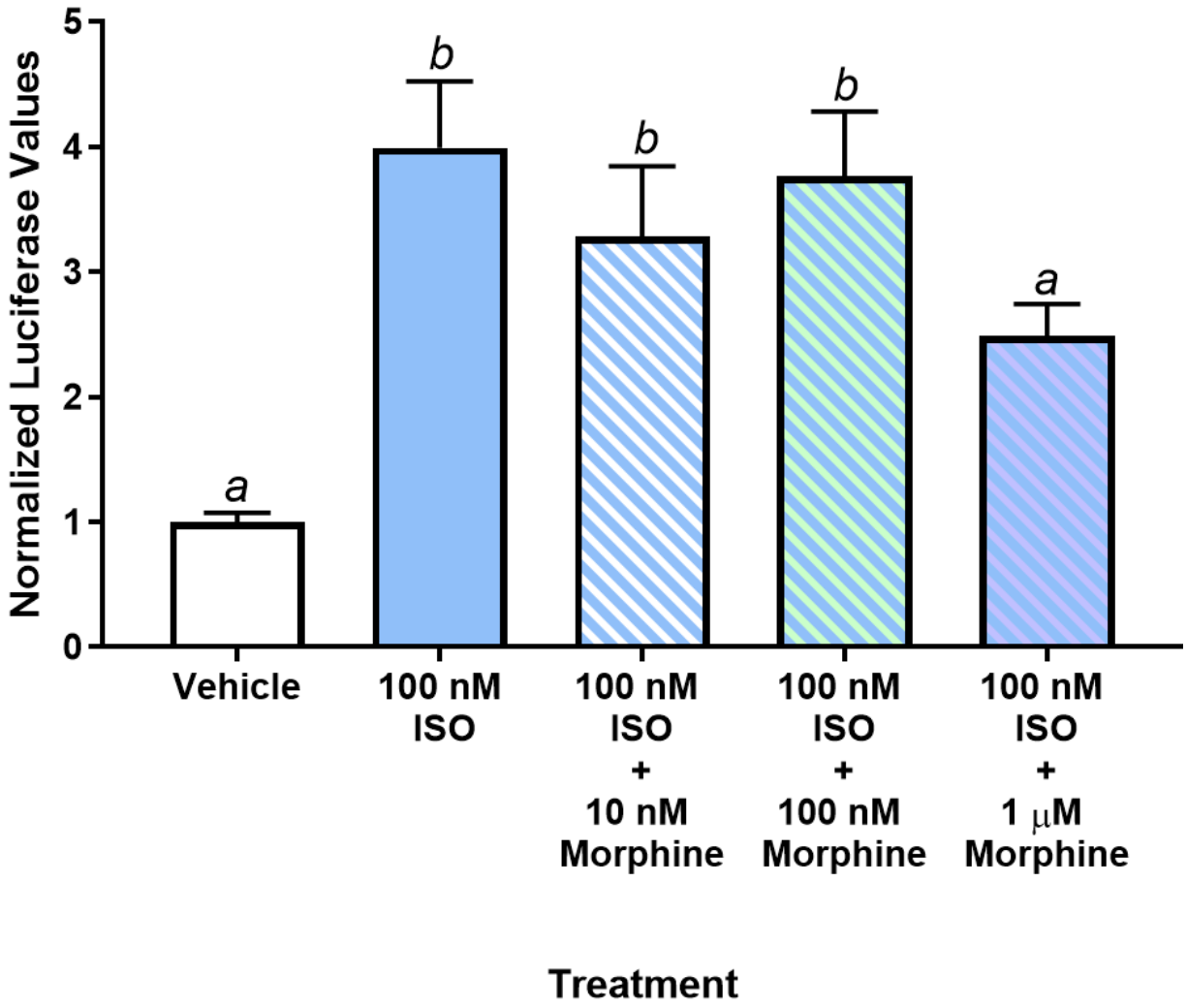

Figure 7: Morphine treatment can attenuate the ISO-induced CRE-luc activation. GT1-7 cells were transfected with CRE-luc and co-treated with 100 nM ISO and morphine for 6 hours. Normalized CRE-luc activation increased with 100 nM ISO treatment, and 10 nM and 100 nM morphine treatments were not enough to alter the 100 nM ISO induced CRE-luc activation. Cotreatment with 100 nM ISO and 1 μM morphine significantly reduced CRE-luc activation compared to the 100 nM ISO treated control. For this experiment, N = 3 and error bars indicate SEM. Data were analyzed with Dunnett's multiple comparison test and "*b*" denotes $p<0.05$ compared to vehicle treatment.

Overexpression of the μOR enhances morphine's effect on CRE-luc activity

To ensure that the morphine-induced decrease in CRE-luc activity was due to μOR activation, we repeated the experiment above with a μOR overexpression vector (abbreviated Oprm1). The cells were treated with the same concentrations of ISO and morphine for 6 hours as the previous experiment. The 100 nM ISO treated cells were co-transfected with CRE-luc/empty vector (abbreviated EV) (average luciferase value 2.11 ± 0.11) or CRE-luc/Oprm1 (average luciferase value 1.91 ± 0.12), and there was no significant difference in CRE-luc activity ($p = 0.99$) (**Figure 8**). The 100 nM ISO and 10 nM morphine-treated cells (CRE-luc/EV: 2.44 ± 0.11 vs. CRE-luc/Oprm1: 1.80 ± 0.08) had significantly reduced CRE-luc activity when overexpressing the μOR ($p = 0.0013$) (**Figure 8**). In the 100 nM ISO and 100 nM morphine-treated cells (CRE-luc/EV: 2.20 ± 0.09 vs. CRE-luc/Oprm1: 1.47 ± 0.06), there was also a significant reduction in CRE-luc activity when the μOR overexpression vector was present ($p = 0.001$) (**Figure 8**). In the cells treated with 100 nM ISO and 1 μM morphine (CRE-luc/EV: 2.31 ± 0.15 vs. CRE-luc/Oprm1: 1.24 ± 0.14), there was a robust reduction in CRE-luc activity ($p = 0.001$) such that there was no significant difference between the CRE-luc/Oprm1 co-transfected 100 nM ISO and 1 μM morphine-treated cells and the vehicle treated cells ($p = 0.99$) (**Figure 8**). All groups were compared with a two-way ANOVA and Sidak's multiple comparisons test (**Table 2**). In summary, there was a robust reduction in CRE-luc activity in the morphine-treated cells co-transfected with the Oprm1 overexpression vector.

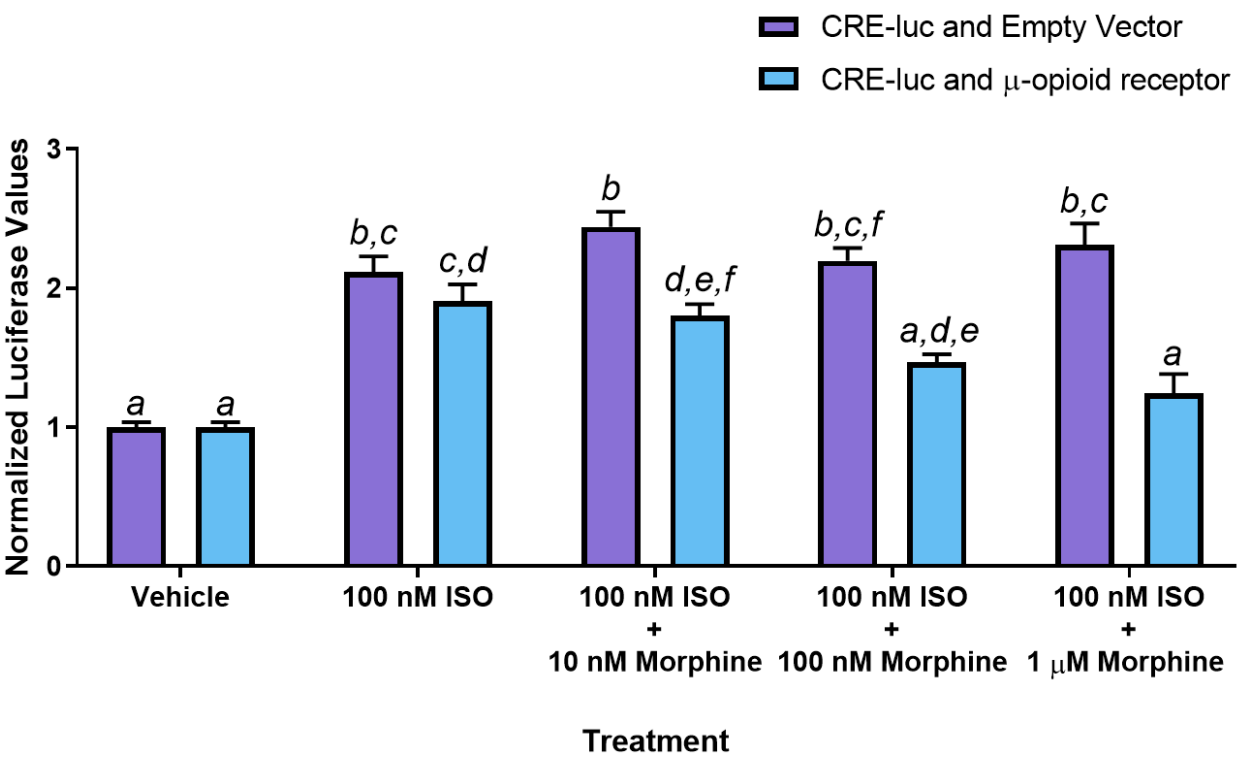

Figure 8: Overexpression of the μOR amplifies morphine inhibitory effect on CRE-luc activation. GT1-7 cells were transfected with a μOR overexpression vector and a CRE-luc reporter vector. Cells were co-treated with 100 nM ISO and morphine for 6 hours. N = 3 and error bars indicate SEM. Data were analyzed with two-way ANOVA and Sidak's multiple comparisons test, where different letters denote $p<0.05$ compared between all groups.

Forskolin robustly activates CRE-luc in a dose-dependent manner

To confirm that our CRE-luc construct was reflecting a change in CRE-luc activity, we tested with an activator of AC, forskolin (FSK). FSK directly activates adenylyl cyclase (AC) to increase cAMP synthesis, which can therefore alter downstream effects of CRE-mediated transcription. GT1-7 cells were treated with 100 nM FSK (average luciferase value: 2.11 ± 0.30), 300 nM FSK (average luciferase value: 2.17 ± 0.32), 1 µM FSK (average luciferase value: 6.37 ± 1.0), 3 µM FSK (average luciferase value: 10.14 ± 1.69), and 10 µM FSK (average luciferase value: 17.17 ± 2.36) for 6 hours (**Figure 9**). There was no difference in CRE-luc activity between the 100 nM FSK ($p = 0.96$) and 300 nM FSK ($p = 0.95$) treated cells and the vehicle treated cells (**Figure 9**). However, 1 µM FSK ($p = 0.019$), 3 µM FSK ($p = 0.0001$), and 10 µM FSK ($p = 0.0001$) treated cells robustly increased CRE-luc activity compared to the vehicle control (**Figure 9**). This illustrates that FSK activates CRE-luc in a dose-dependent manner.

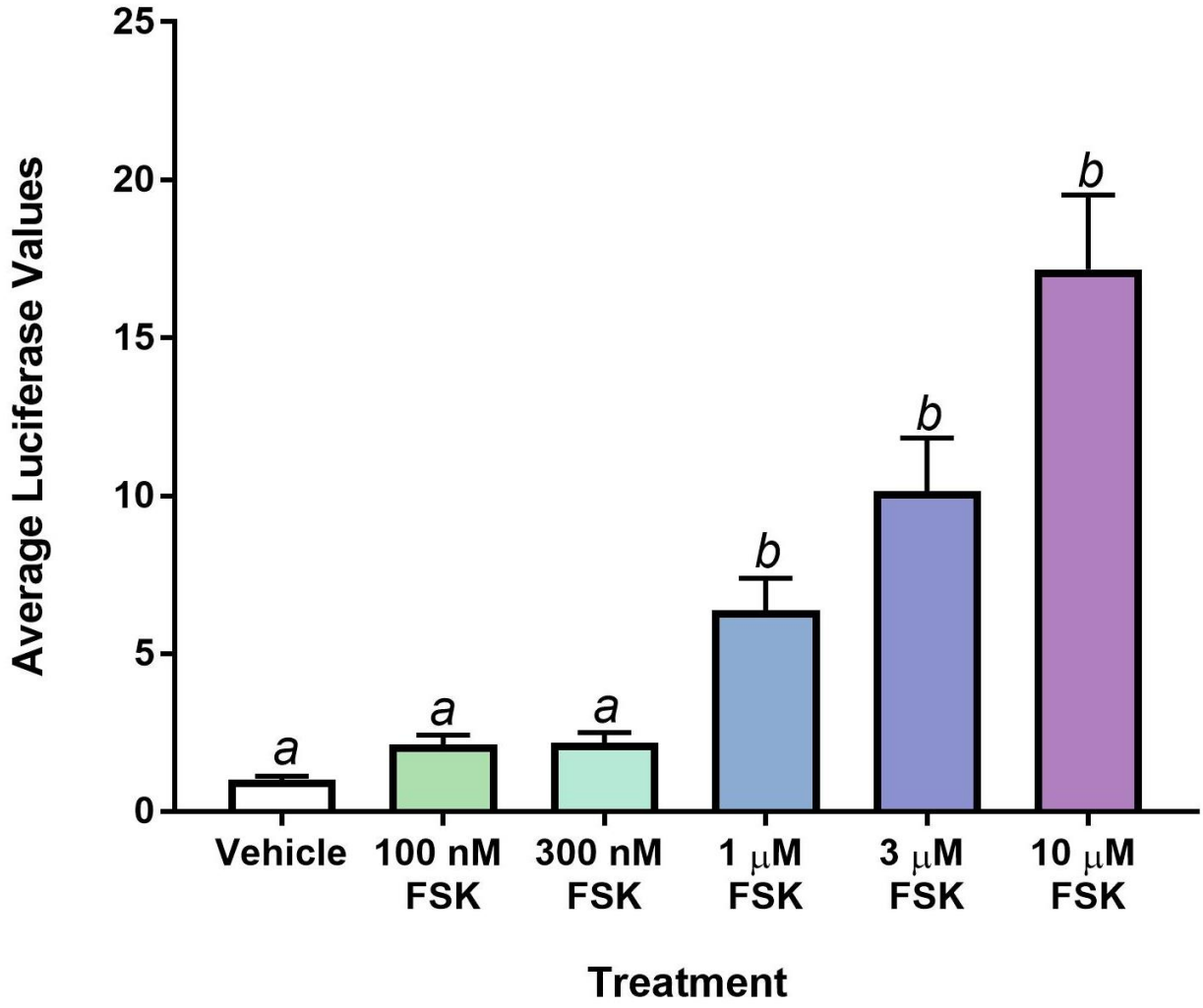

Figure 9: FSK robustly activates CRE-luc in a dose-dependent manner. GT1-7 cells were treated with FSK for 6 hours. N = 3 and error bars indicate SEM. Data were analyzed with one-way ANOVA and Dunnett's multiple comparison test, where "*b*" indicates $p<0.05$ compared to vehicle control.

Morphine co-treatment did not affect FSK-induced CRE-luc activity

After the FSK dose response curve was conducted, 1 µM FSK was chosen as the optimal concentration for inducing CRE-luc activity (average luciferase value: 6.21 ± 0.51) (**Figure 10**). Transfected GT1-7 cells were co-treated with 1 µM FSK and 3 different morphine concentrations (1 µM FSK + 10 nM morphine: 5.99 ± 1.42; 1 µM FSK + 100 nM morphine: 5.93 ± 0.44; 1 µM FSK + 1 µM morphine: 6.56 ± 0.97) for 6 hours (**Figure 10**). Dunnett's multiple comparisons test was conducted to compare luciferase averaged values to the vehicle control (vehicle vs. 1 µM FSK: $p = 0.0003$; vehicle vs. 1 µM FSK + 10 nM morphine: $p = 0.0004$; vehicle vs. 1 µM FSK + 100 nM morphine: $p = 0.0006$; vehicle vs. 1 µM FSK + 1 µM morphine: $p = 0.0001$) (**Figure 10**). There was no significant difference in CRE-luc activity found between the 1 µM FSK treated cells and the morphine and FSK cotreated cells.

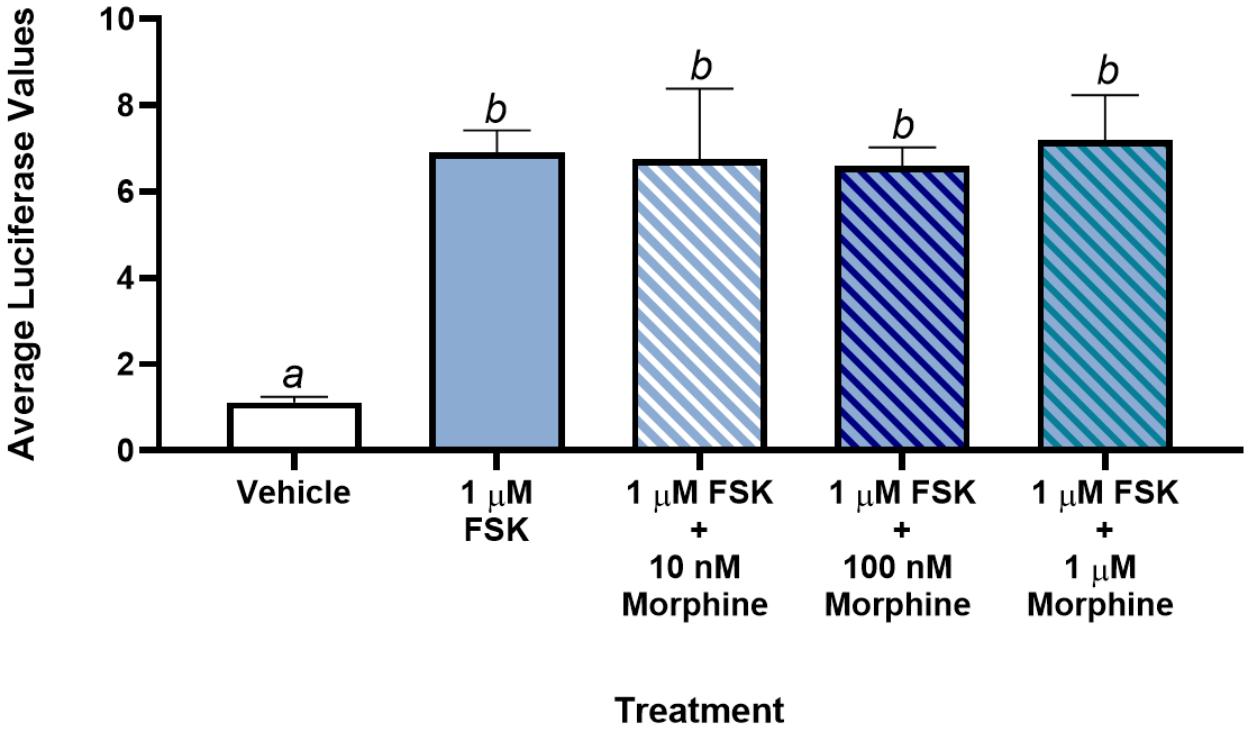

Figure 10: FSK and morphine cotreatment does not alter CRE-luc activity. GT1-7 cells were cotreated with FSK and increasing concentrations of morphine for 6 hours. N = 3 and error bars indicate SEM. Data were analyzed with Dunnett's multiple comparison test and "*b*" indicates $p < 0.05$ compared to vehicle treated control.

Overexpression of μOR in GT1-7 cells enables morphine's inhibitory effect on CRE-luc activity

To ensure that morphine was acting through the μOR, we transfected the GT1-7 cells with the CRE-luc and an overexpression vector (Oprm1). The cells were cotreated with 1 μM FSK and increasing concentrations of morphine for 6 hours. The 1 μM FSK treated cells were co-transfected with CRE-luc/EV (average luciferase value 3.41 ± 0.19) or CRE-luc/Oprm1 (average luciferase value 3.44 ± 0.39), and there was no significant difference in CRE-luc activity ($p > 0.99$) when the μOR was overexpressed (**Figure 11**). The 1 μM FSK and 10 nM morphine cotreated cells (CRE-luc/EV: 3.21 ± 0.18 vs. CRE-luc/Oprm1: 2.66 ± 18) had similar CRE-luc activity when overexpressing the μOR ($p = 0.97$) (**Figure 11**). In the 1 μM FSK and 100 nM morphine cotreated cells (CRE-luc/EV: 3.44 ± 0.26 vs. CRE-luc/Oprm1: 2.21 ± 0.18), there was a significant reduction in CRE-luc activity when the μOR overexpression vector was present ($p = 0.005$) (**Figure 11**). In the cells cotreated with 1 μM FSK and 1 μM morphine (CRE-luc/EV: 3.46 ± 0.33 vs. CRE-luc/Oprm1: 1.74 ± 0.05), there was a significant reduction in CRE-luc activity ($p < 0.0001$) such that there was no significant difference between the CRE-luc/Oprm1 co-transfected 1 μM FSK + 1 μM morphine cotreated cells and the vehicle treated cells ($p = 0.54$) (**Figure 11**). In summary, the presence of the Oprm1 overexpression vector caused a dose-dependent reduction in FSK-induced CRE-luc activity when cotreated with morphine.

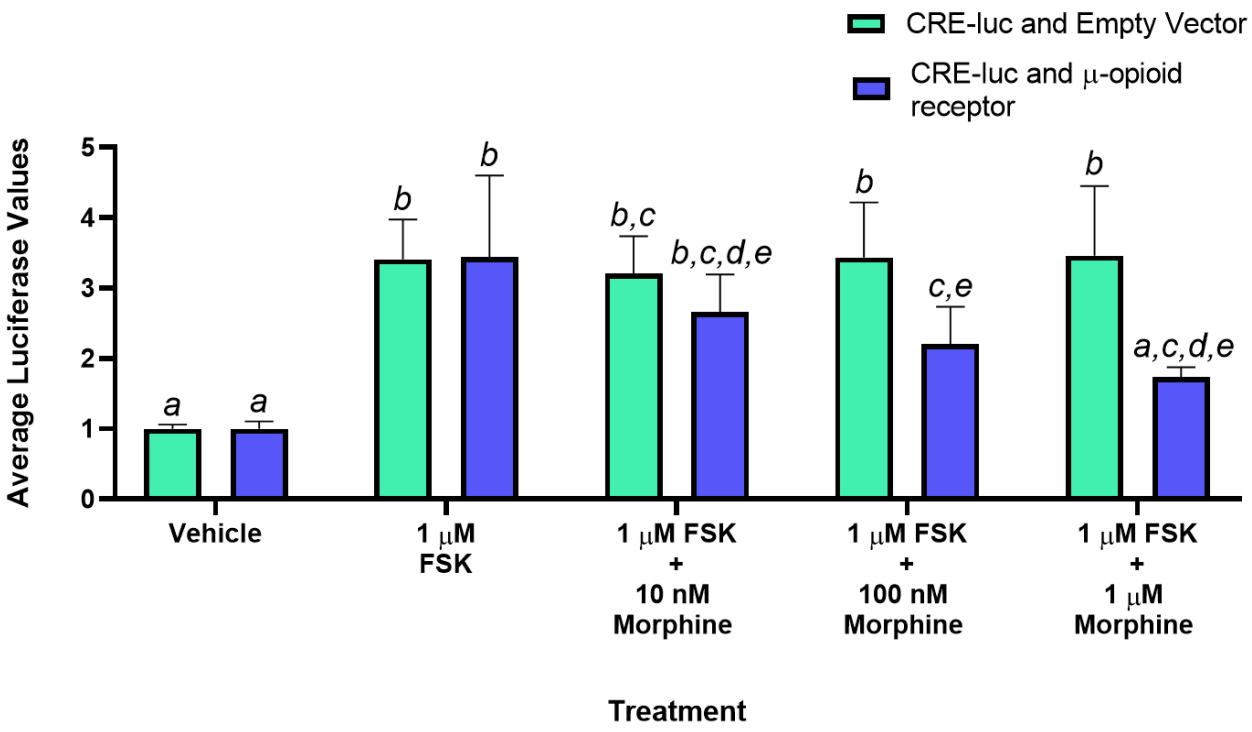

Figure 11: Overexpression of μOR enhances morphine's inhibitory effect in a dose-dependent manner. GT1-7 cells were co-transfected with CRE-luc and a μOR expression vector or respective empty vector. Cells were cotreated with 1 μM FSK and morphine for 6 hours. N = 3 and error bars indicate SEM. Data were analyzed with two-way ANOVA and Sidak's multiple comparisons test, where different letters denote $p<0.05$ compared between all groups.

CHAPTER II: Morphine alters GnRH responsiveness through μOR activation

Previous studies have established that morphine treatment causes a decrease in GnRH activity, resulting in decreased LH secretion (11). We hypothesized that morphine treatment in mice altered GnRH responsiveness via μOR activation in GnRH neurons.

Morphine-treated female mice have a significant decrease in mean LH secretion

First, we wanted to see if morphine treatment could reduce LH secretion in mice. We were kindly gifted ovariectomized female mice by the Breen Church Lab. Ovariectomized females do not produce E_2, effectively lifting E_2's negative feedback effect on the HPG axis. This results in a rise in basal LH pulses that we can more easily measure. We injected 4 females with morphine and 4 females with saline at time 0, and blood was collected every 6 minutes for 60 minutes. Serum was extracted from the blood and measured for LH. Saline-treated mice had normal, rapid LH pulses while the morphine-treated mice had slower and fewer LH pulses (**Figure 12A**). We took the mean LH concentration over 60 minutes and found that morphine-treated mice had significantly reduced LH secretion (saline: 3.35 ± 0.0003 ng/mL vs. morphine: 2.37 ± 0.19 ng/mL; $p = 0.000271$) (**Figure 12B**). This illustrates that morphine can suppress pulsatile LH secretion in ovariectomized female mice.

Figure 12: Morphine treatment reduces mean LH secretion. 8 wildtype female mice were ovariectomized. Mice were treated with 20 mg of morphine/kg of mouse or saline. Blood was collected via tail bleed every 6 minutes for 60 minutes. **Panel A** illustrates representative LH pulse graphs for the saline and morphine-treated females. **Panel B** shows the measured mean LH secreted from the morphine and saline treated female mice. For this experiment, n = 4 per treatment group and error bars indicate SEM. Data were analyzed with student's t-test, where " * " $p<0.05$ compared to saline control.

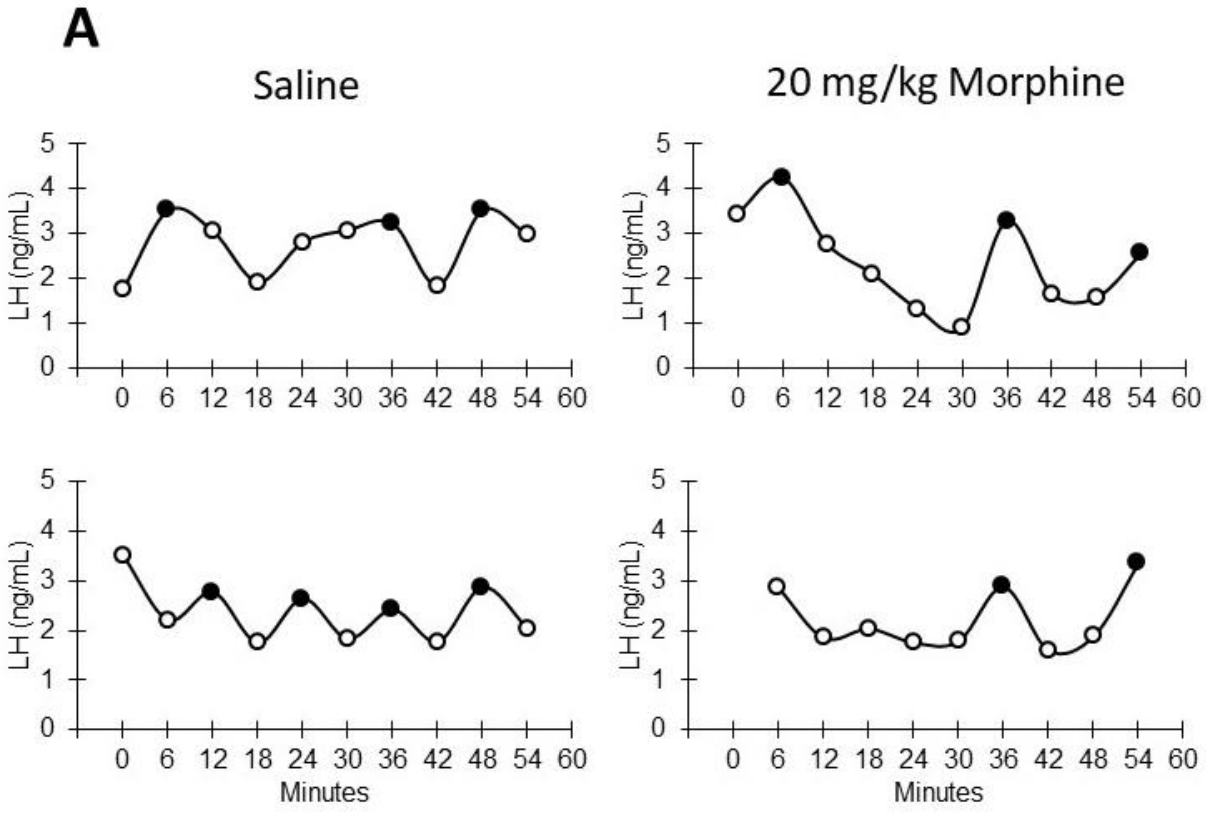
A
Saline
20 mg/kg Morphine
LH (ng/mL)
0 1 2 3 4 5
0 6 12 18 24 30 36 42 48 54 60
Minutes

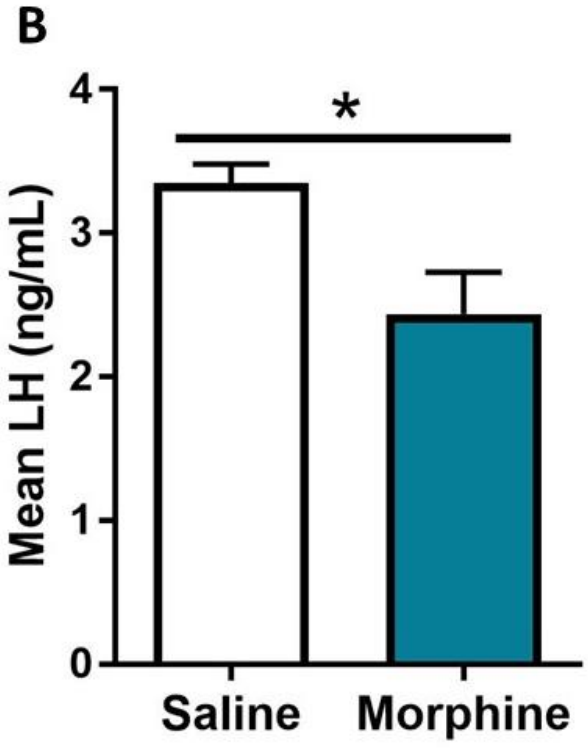
B
Mean LH (ng/mL)
0 1 2 3 4
*
Saline
Morphine

Preliminary data illustrate that morphine pretreatment cannot inhibit GnRH-induced LH secretion

Next, we wanted to see if morphine could alter GnRH-induced LH secretion. Previous studies show that opioids act on the hypothalamus to suppress the HPG axis (12). However, to rule out opioid action on the pituitary, we conducted a GnRH challenge. Exogenous GnRH can be given to activate the anterior pituitary and induce LH secretion. Female mice were pretreated with morphine or saline 15 minutes prior to a bolus of exogenous GnRH (1µg/kg). Blood was collected immediately before and 15 minutes after GnRH treatment to measure LH before and after induction. Preliminary data suggest that morphine pretreatment does not reduce GnRH-induced LH secretion (saline pretreatment: pre-GnRH: 22.01 ± 4.38 pg/mL vs. post-GnRH: 212.86 ± 138.19 pg/mL; morphine pretreatment: pre-GnRH: 34.957 ± 17.33 pg/mL vs. post-GnRH: 170.55 ± 68.4 pg/mL) (**Figure 13**). These findings indicate that morphine suppression of the HPG axis does not occur at the level of the pituitary.

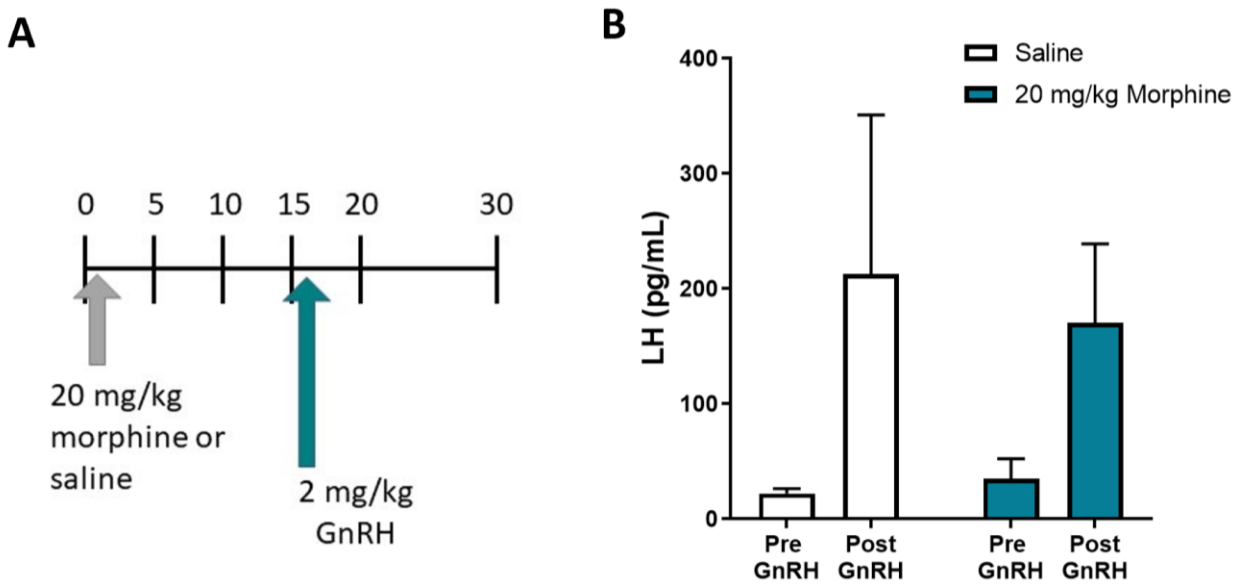

Figure 13: Morphine pretreatment fails to inhibit GnRH-induced LH release. Female mice were pretreated with saline or morphine. Blood was collected 15 minutes later, and GnRH was intraperitoneally injected. Blood was collected again 15 minutes later. For this experiment, n = 3 per treatment group and error bars indicate SEM. Data were analyzed with one-way ANOVA, where " * " $p<0.05$ compared to saline control.

Morphine pretreatment inhibits kisspeptin-induced LH secretion when the μOR is present in GnRH neurons

Since morphine action on the pituitary is not responsible for decreased LH secretion, we decided to look upstream of the pituitary and study GnRH neurons. Exogenous kisspeptin can be used to activate GnRH neurons and induce LH secretion. WT female mice were pretreated with morphine or saline, and then given kisspeptin. Blood was collected pre- and post- KISS1 treatment to measure LH secretion. As expected, we found that mice pretreated with saline had increased LH secretion after kisspeptin treatment (WT mice saline pretreatment: pre-kisspeptin: 149.87 ± 55.49 pg/mL vs. post-kisspeptin: 1066.48 ± 222.15 pg/mL; pre- vs. post- kisspeptin, $p = 0.004$) (**Figure 14**). However, there was no significant difference in LH found between pre- and post- kisspeptin treatment in the morphine pretreated mice (WT mice morphine pretreatment: pre-kisspeptin: 191.69 ± 34.77 pg/mL vs. post-kisspeptin: 513.72 ± 157.06 pg/mL; pre- vs. post- kisspeptin, $p = 0.08$) (**Figure 14**). This illustrates that morphine pretreatment attenuates GnRH neuron responsiveness to kisspeptin.

To see if this attenuation in GnRH neuron responsiveness was due to μOR activation, we created mice that lacked the μOR in GnRH neurons using Cre-Lox P technology called *Oprm1* GnRH KO mice. We created the *Oprm1* GnRH KO mice by crossing an *Oprm1*$^{flox/flox}$ mouse (21) with a LHRH Cre mouse (22). The *Oprm1* GnRH KO mice were pretreated with morphine and underwent the kisspeptin challenge. We found a significant increase in LH after kisspeptin treatment, indicating morphine pretreatment did not attenuate GnRH neuron responsiveness to kisspeptin (*Oprm1* GnRH KO mice morphine pretreatment: pre-kisspeptin: 95.18 ± 15.86 pg/mL vs. post-kisspeptin: 700.47 ± 162.51 pg/mL; pre- vs. post-kisspeptin, $p = 0.02$) (**Figure 14**).

These findings suggest that morphine's suppressive effects are mediated via μOR activation in GnRH neurons.

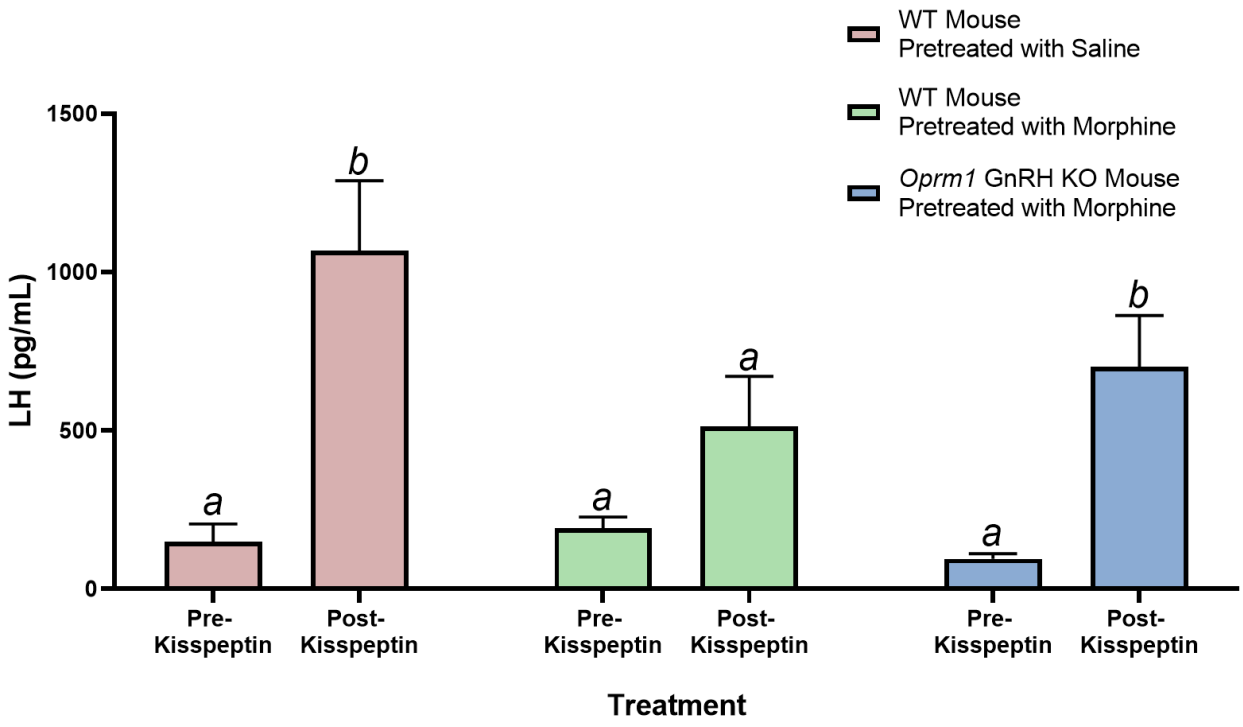

Figure 14: Morphine pretreatment attenuates kisspeptin-induced LH secretion only when the μOR is expressed in GnRH neurons. WT mice were pretreated with saline (n = 8) or morphine (n = 8), and then given KISS1 to induce LH secretion. Mutant mice were pretreated with morphine (n = 5) and then treated with kisspeptin. Kisspeptin was able to induce LH secretion in WT saline pretreated mice and mutant morphine pretreated mice. Morphine pretreatment in WT animals attenuated the kisspeptin-induced LH secretion. Data show average and error bars illustrate SEM. Data were analyzed by two-way ANOVA and Sidak's multiple comparison's test, where "*b*" denotes a significant difference compared to pre-kisspeptin LH concentrations.

CHAPTER III: Chronic morphine treatment does not alter gene expression in the ovaries, pituitary, or hypothalamus

Since acute morphine alters kisspeptin-induced LH secretion, we wanted to see if chronic morphine could alter gene expression. We chronically treated WT female mice with increasing amounts of morphine, and harvested the ovaries, pituitary, and hypothalamus. All tissue was turned into RNA and cDNA for quantitative PCR analysis (qPCR).

In the hypothalamus, we examined average fold change in gene expression of *GnRH*, *Oprm1* (the gene for the μOR), and *GPR54* (the gene for Kisspeptin receptor). While there was no significant difference in *GnRH* expression found between the saline treated mice and the morphine-treated mice (saline: 1.03 ± 0.14 vs. morphine: 0.56 ± 0.17; $p = 0.07$), there was a trend towards a decrease in *GnRH* expression (**Figure 15**). When looking at *Oprm1* gene expression, there was no significant difference found between the saline treated and morphine-treated mice (saline: 1.05 ± 0.24 vs. morphine: 0.87 ± 0.10; $p = 0.46$) (**Figure 15**). There was also no significant difference in *GPR54* gene expression between the saline treated and morphine-treated mice (saline: 1.01 ± 0.08 vs. morphine: 2.65 ± 1.05; $p = 0.15$).

For the pituitary, we analyzed average fold change in gene expression of the beta subunit of LH and FSH, *LHβ* and *FSHβ.* We found no significant difference in gonadotropin expression between the saline and morphine-treated animals (*LHβ:* saline: 1.04 ± 0.11 vs. morphine: 0.74 ± 0.06, $p = 0.06$; *FSHβ:* saline: 1.21 ± 0.27 vs. morphine: 0.82 ± 0.18, $p = 0.31$) (**Figure 16**).

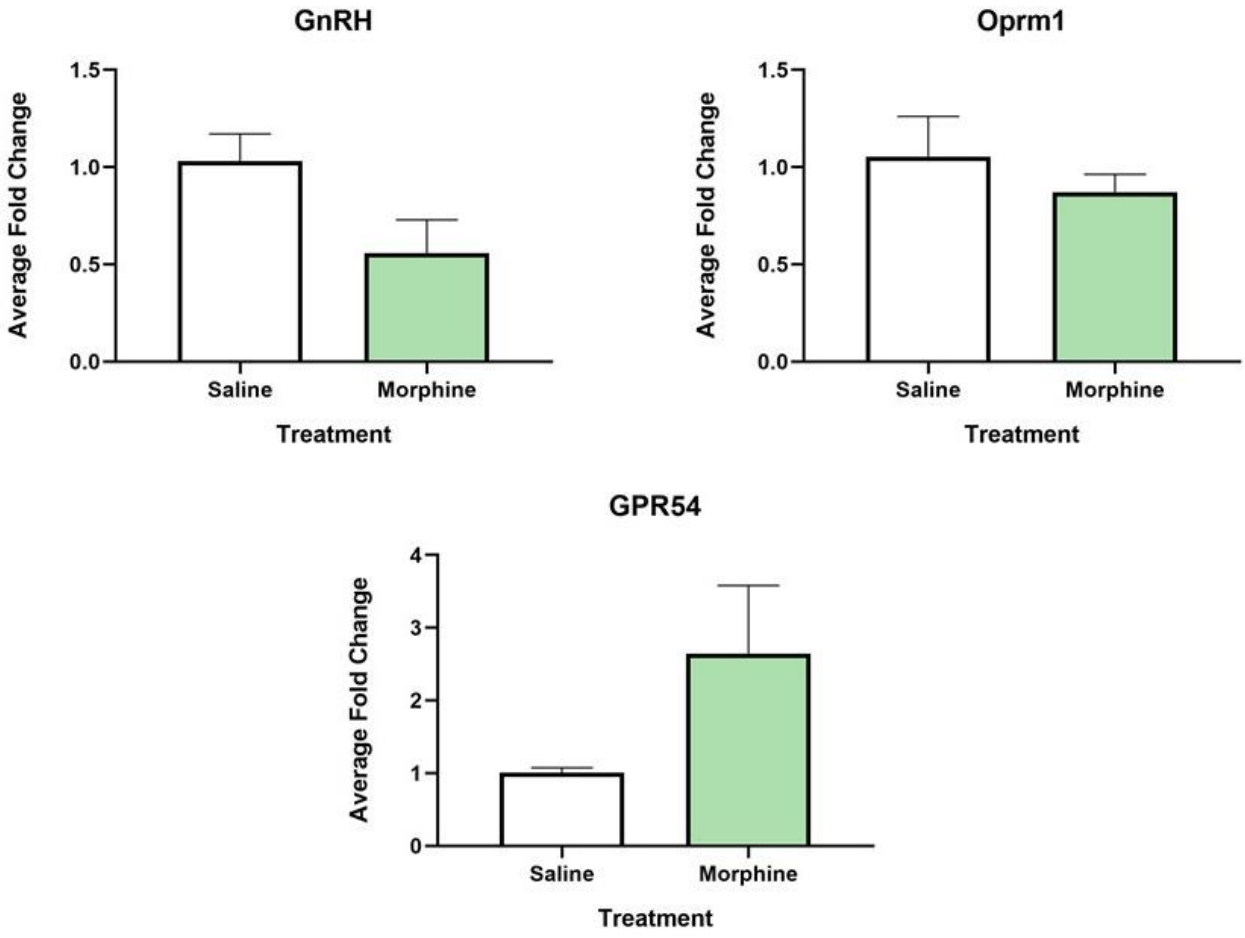

Figure 15: Chronic morphine treatment does not alter gene expression in the hypothalamus. The hypothalami from chronic morphine-treated and saline-treated mice were separated, RNA was isolated, and cDNA was made. qPCR was run for *GnRH* (n = 5), *Oprm1* (n = 5), and *GPR54* (n = 5) gene expression. There was no significant difference found between the saline-treated mice and the morphine-treated mice. Data were analyzed with student's t-test, where "*" denotes $p < 0.05$.

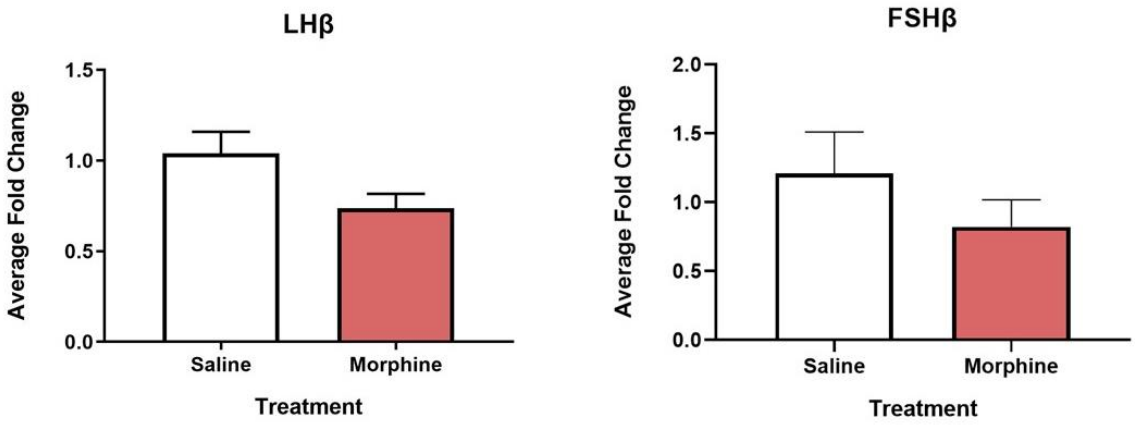

Figure 16: Chronic morphine treatment did not alter pituitary gene expression. The pituitary from chronic morphine-treated and saline-treated mice were separated, RNA was isolated, and cDNA was made. qPCR was run for *LHβ* (n = 6) and FSH*β* (n = 6) gene expression. There was no significant difference found between the saline-treated mice and the morphine-treated mice in either gene. Data were analyzed with student's t-test, where "*" denotes $p < 0.05$.

We chose to analyze *LH-R, FSH-R, STAR, AMH,* and *Cyp19a1* gene expression changes in the ovaries. The genes *LH-R* and *FSH-R* code for gonadotropin receptors that regulate gonadotropin responsiveness in the gonads. We found no significant difference between the saline treated and morphine-treated mice in either gene (*LH-R*: saline: 1.19 ± 0.34 vs. morphine: 0.39 ± 0.03, p = 0.07; *FSH-R*: saline: 1.1 ± 0.22 vs. morphine: 0.74 ± 0.25; p = 0.31) (**Figure 17**). The *STAR* gene codes for Steroidogenic Acute Regulatory protein (STAR), an integral transport protein in the rate-limiting step of steroid synthesis. There was no significant difference in *STAR* expression between the control and morphine mice (saline: 1.47 ± 0.50 vs. morphine: 0.81 ± 0.21, p = 0.26) (**Figure 17**). The *AMH* gene codes for Anti-Müllerian Hormone (AMH), a hormone that regulates folliculogenesis in the ovaries. We found no significant difference between the control and morphine-treated mice (saline: 1.10 ± 0.22 vs. morphine: 0.73 ± 0.06, p = 0.16) (**Figure 17**). The gene *Cyp19a1* codes for the enzyme aromatase, which is responsible for converting androgens to estrogen. There was no significant difference found between the

saline and morphine-treated mice (saline: 5.60 ± 2.8 vs. morphine: 4.03 ± 2.79, p = 0.70) (**Figure 17**).

Figure 17: There was no significant difference in ovarian gene expression after chronic morphine treatment. Ovaries from chronic morphine-treated and saline-treated mice were separated, RNA was isolated, and cDNA was made. qPCR was run for *LH-R* (n = 5), *FSH-R* (n = 5), *STAR* (n = 6), *AMH* (n = 6), and *Cyp19a1* (n = 6) gene expression. There was no significant difference found between the saline-treated mice and the morphine-treated mice in either gene. Data were analyzed with student's t-test, where "*" denotes $p < 0.05$.

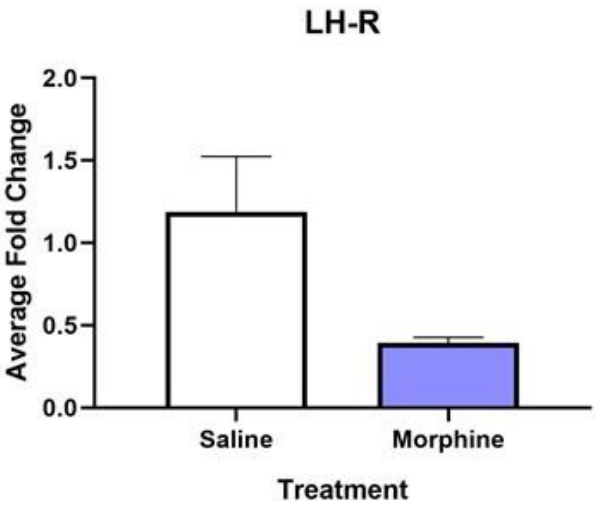
LH-R
Average Fold Change
2.0
1.5
1.0
0.5
0.0
Saline
Morphine
Treatment

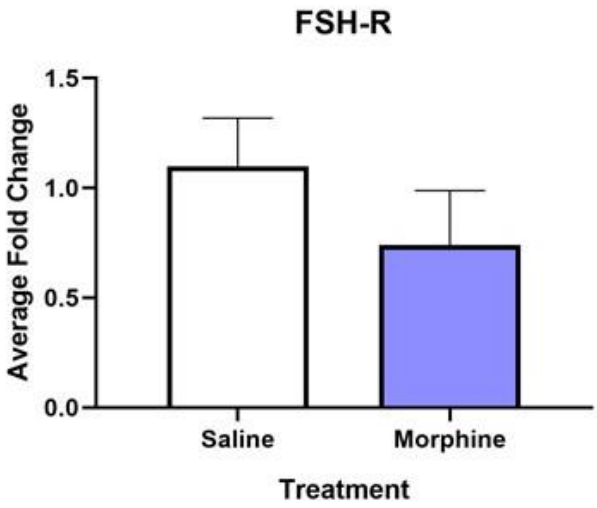
FSH-R
Average Fold Change
1.5
1.0
0.5
0.0
Saline
Morphine
Treatment

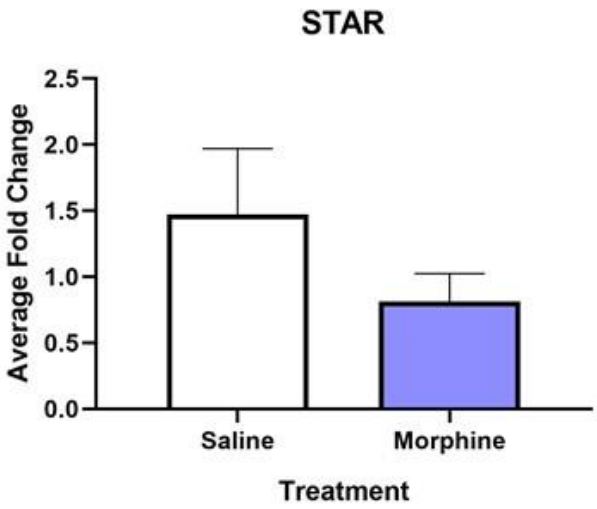
STAR
Average Fold Change
2.5
2.0
1.5
1.0
0.5
0.0
Saline
Morphine
Treatment

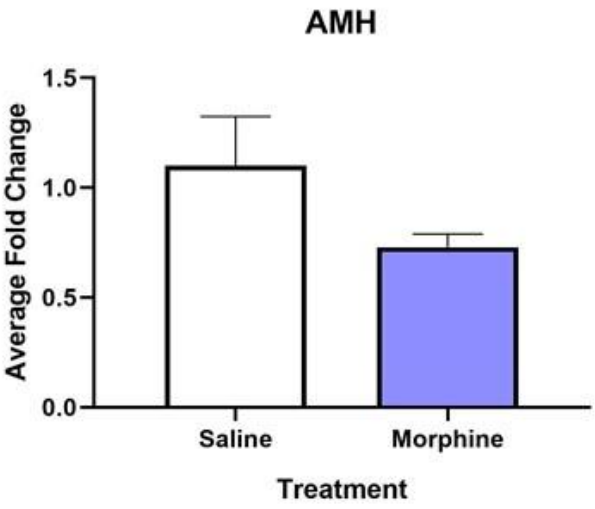
AMH
Average Fold Change
1.5
1.0
0.5
0.0
Saline
Morphine
Treatment

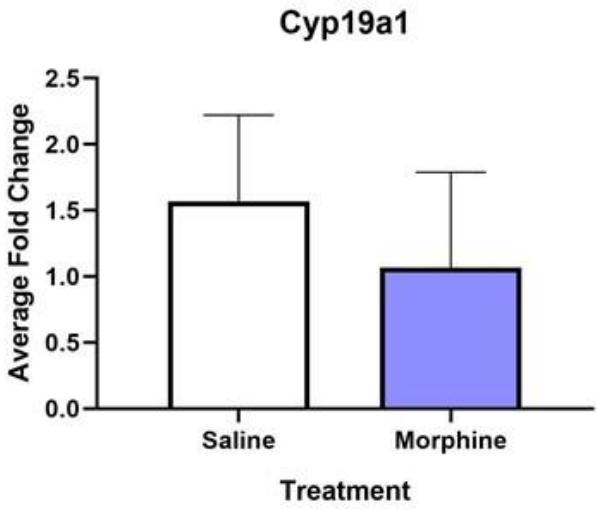
Cyp19a1
Average Fold Change
2.5
2.0
1.5
1.0
0.5
0.0
Saline
Morphine
Treatment

DISCUSSION

Morphine treatment decreases cAMP signaling in immortalized GnRH neurons

Opioid use suppresses the hypothalamic-pituitary-gonadal axis to cause OIH, which is associated with μOR activation and reduced LH secretion (11). While not much is known about the exact mechanism of OIH, we have discovered a potential key aspect of this mechanism. Previous studies have shown morphine to decrease the electrical activity that drives GnRH activity (11), highlighting that GnRH neurons play a key role in the development of OIH.

We have demonstrated, using immortalized GnRH neurons, that GnRH neurons express functional μOR (**Figure 4**) and are therefore susceptible to opioid action. The μOR is an inhibitory G-protein coupled receptor, where activation of the μOR leads to a decrease in cAMP synthesis (13). The reduction in cAMP leads to a reduction in downstream activity such as reduced PKA activity, CREB phosphorylation, and CRE-mediated transcription in various promoter regions (13). Zhang and colleagues were able to identify multiple half CRE sites on the GnRH promoter regions of rats and humans (24), illustrating a potential mechanism of GnRH regulation through cAMP signaling. When CREB is selectively deleted in GnRH neurons, mice are infertile (25), and when the CRE site on the human GnRH promoter is mutated, there is reduced basal GnRH promoter activity (26). On the other hand, when increasing cAMP synthesis through forskolin treatment, *GnRH* transcription *in vivo* and *cfos* transcription *in vitro* increase (27). These findings highlight the importance of cAMP signaling in GnRH neurons in maintaining normal fertility, and how morphine may reduce GnRH activity to cause OIH.

The use of luciferase reporter assays to characterize G-protein coupled receptor pathways was implemented to measure cAMP signaling in immortalized GnRH neurons (28). *In vitro*, we

have demonstrated that we are able to measure CRE-mediated transcription through a CRE-luciferase (CRE-luc) reporter vector by measuring CRE-luc transcription (**Figure 6**). To test the CRE-luc, we treated the transfected GT1-7 cells with drugs known to increase cAMP synthesis, isoproterenol (ISO) and forskolin (FSK) and found that CRE-luc activity increased in a dose-dependent manner (**Figure 6 and 9**). Previously, FSK was shown to increase *cfos* transcription, illustrating increased neuronal activity, and GnRH secretion in GT1-7 cells (27). The increased GnRH neuronal activity may demonstrate the stimulatory effects of FSK, and therefore increased cAMP, on the HPG axis. Next, to show the inhibitory effects of opioids, the transfected cells were cotreated with ISO or FSK and morphine, where morphine was able to attenuate ISO-induced CRE-luc activation but not FSK-induced activity in GT1-7 cells (**Figure 7 and 10**). Since FSK directly activates adenylyl cyclase to increase cAMP, while ISO indirectly increases cAMP, the transduction speed in cAMP synthesis may play a role in CRE-mediated transcription. Morphine pretreatment has been shown to decrease GnRH secretion in GT1-7 cells (29), and the decreased CRE-luc activity may play a role in this altered GnRH responsiveness.

Morphine has been shown to bind to and activate the μOR; however, morphine is able to bind to the κOR and the δOR with extremely low affinity (30). To verify the role of the μOR in the reduced CRE-luc activity, an overexpression experiment was performed where GT1-7 cells were co-transfected with CRE-luc and a μOR expression vector, and then cotreated with ISO or FSK and morphine. The presence of the overexpression vector enhanced morphine's inhibitory effect on CRE-luc activation, such that morphine cotreatment with FSK or ISO was able to decrease CRE-luc activation (**Figure 8 and 11**). This therefore verified that the inhibitory effects of morphine were mediated by μOR activation. Future studies will confirm the role of μOR using DAMGO, a more specific μOR agonist.

Morphine treatment decreases GnRH responsiveness in a mouse model

Previous studies in mammals illustrate that morphine treatment decreases LH secretion from the pituitary (11); however, this characteristic is not well studied in mice. We have shown that morphine treatment decreases LH pulsatility and mean basal LH secretion in ovariectomized females (**Figure 12**). Due to the low concentrations of basal LH and sensitivities of current assays that measure LH, LH pulse measurements are usually not taken from intact animals (31). By ovariectomizing the female mice, they are unable to make estrogen, and the negative feedback on the hypothalamus and pituitary are lifted. This ensures that the mice secrete pulsatile LH at measurable levels. The results from the morphine-treated mice correlate with opioid studies done in other animal models (11), where morphine reduces both number of LH pulses and mean LH secretion.

The *in vitro* data from GT1-7 cells above strongly suggest that GnRH neurons play a role in the decreased LH secretion that ultimately leads to the development of OIH. To see if morphine could alter GnRH responsiveness, a kisspeptin hormone challenge was performed where WT mice were pretreated with morphine or saline. Kisspeptin treatment activates GnRH neurons, causing an increase in downstream LH secretion (32), as seen in the saline treated WT mice. On the other hand, morphine pretreated WT mice had reduced post-kisspeptin LH secretion (**Figure 14**). This illustrates that kisspeptin was unable to properly activate the GnRH release after morphine treatment, therefore altering GnRH neuron responsiveness. While previous studies have implicated the hypothalamus as the main site of opioid action in the development of OIH (14, 15, 16), the presence of the μOR in the anterior pituitary (33) implies a potential site for opioid action. To address this, we performed a GnRH hormone challenge after morphine or saline pretreatment to measure pituitary responsiveness. Preliminary data showed

that morphine pretreated mice were able to respond to stimulatory GnRH by increasing LH secretion (**Figure 13**). This demonstrates that morphine did not alter pituitary responsiveness to GnRH, and that morphine most likely does not suppress the HPG axis at the level of the pituitary.

Due to decreased GnRH responsiveness from morphine treatment, we wanted to verify the role the μOR activation played in the GnRH neurons. We created a mutant mouse model by selectively deleting the gene that codes for the μOR, *Oprm1*, in GnRH neurons by crossing an $Oprm1^{flox/flox}$ mouse (21) with an LHRH-Cre mouse (22). Previous studies have shown that the LHRH-Cre mouse has better selectivity for GnRH neurons than the GnRH-Cre (34). While the GnRH-Cre is expressed in more GnRH neurons, it also affects many non-GnRH populations (34). Therefore, deletion of *Oprm1* in GnRH neurons occurs more accurately with the LHRH-Cre expression. After creating these mice, we performed the kisspeptin challenge after morphine or saline pretreatment. Once the μOR was selectively deleted in GnRH neurons, the mice pretreated with morphine were able to respond to kisspeptin with increased LH secretion (**Figure 14**). This indicates that the lack of μOR enabled GnRH neurons to respond to kisspeptin even after morphine pretreatment. Therefore, the presence of μOR in GnRH neurons is integral to morphine's effect on altering GnRH responsiveness. Future studies will confirm Oprm1 knockout in GnRH neurons using PCR, and examine GnRH pulses in these mice, as endogenous opioids are believed to play a role in regulating GnRH release.

Chronic morphine exposure did not alter hypothalamic, pituitary, or ovarian gene expression

While acute morphine use has been shown to decease LH and sex steroid secretion (35), chronic morphine use leads to tolerance and altered gene expression in rats (36). To see if morphine tolerance would lead to changes in gene expression in mice, we induced tolerance by chronically treating mice with increasing concentrations of morphine for 7 days. We isolated RNA from the hypothalamus, pituitary, and ovaries and made cDNA to run qPCR for select genes.

In the hypothalamus, we looked for altered *GnRH, Oprm1*, and *GPR54* gene expression. Previous studies have found chronic morphine treatment to significantly decrease *GnRH* expression and biosynthesis in rats (37). While the difference between the saline treated and morphine-treated mice was trending towards significance ($p = 0.07$), we found no significant alteration in *GnRH* gene expression after chronic morphine treatment (**Figure 15**). Differential promoter regulation between species, for example the lack of CRE sites in the mouse *GnRH* promoter region, may play a role in the lack of altered *GnRH* expression in the chronically treated mice (24). Chronic morphine treatment is also known to upregulate general *Oprm1* expression in the rat brain (36) but downregulate *Oprm1* expression in the hypothalamus of guinea pigs (38). In contrast, we found no significant difference in *Oprm1* expression after 7 days of morphine treatment (**Figure 15**). This may be due to length of treatment; the rats were treated for 10 days and the guinea pigs for 8 days (36, 38). In addition, downregulation was seen in the arcuate nucleus of the hypothalamus in guinea pigs, while we looked at whole hypothalamic gene expression. Due to the scope of tissue collected, *Oprm1* gene expression may have been altered in different areas of the hypothalamus, which would have leveled out to a

general lack of change when looking at the whole hypothalamus. When we looked at *GPR54* gene expression, the gene encoding for the kisspeptin receptor, we found no significant difference between the morphine-treated animals and the saline treated animals (**Figure 15**). This finding coincided with the literature, where *GPR54* expression was not altered but *KISS1* expression was (39). This indicates that GnRH neuron responsiveness to KISS1 was not altered via differential receptor regulation.

In the pituitary, we looked for altered *LHβ* and *FSHβ* gene expression. Since morphine is known to decrease LH secretion 11, we wanted to see if morphine could alter its expression as well. We found that *LHβ* expression trended towards a decrease ($p = 0.06$) while there was no change in *FSHβ* gene expression (**Figure 16**). The lack of change in *FSHβ* gene expression agrees with previous literature that found no changes in FSH secretion after chronic morphine treatment (40). These findings indicate that altered LH secretion plays a more important role in the decrease in sex steroid production in the mouse.

In the ovaries, we looked for altered *LH-R*, *FSH-R*, *STAR*, *AMH*, and *Cyp19a1* gene expression. We found no change in *LH-R* gene expression nor in *FSH-R* gene expression, indicating that ovary responsiveness to the gonadotropins was not altered by morphine treatment (**Figure 17**). These findings suggest that LH and FSH signaling was unaffected by chronic morphine treatment. Also, we found no change in *STAR* gene expression after chronic morphine treatment (**Figure 17**). The *STAR* gene codes for an important protein that regulates cholesterol transport into the mitochondria, a necessary step for steroidogenesis (41). This indicates that chronic morphine treatment does not change cholesterol transport to the mitochondria, allowing this step of steroidogenesis to occur unaltered. In addition, we found that *AMH* gene expression was trending towards a decrease ($p = 0.06$) after chronic morphine treatment (**Figure 17**). AMH

is a necessary hormone that regulates follicle maturation. Previous studies have found that chronic morphine treatment causes a reduction in the number of follicles (42), which may have occurred due to downregulated *AMH* gene expression. Finally, we saw no significant difference in *Cyp19a1* gene expression (**Figure 17**). *Cyp19a1* codes for the enzyme aromatase, which is responsible for the conversion of androgens to estrogens (43). Previous findings have shown upregulation of *Cyp19a1* gene expression in male rats after chronic morphine treatment (44), indicating a potential sexual dimorphism to how chronic morphine alters gonadal regulation of sex steroids.

Overall, these findings implicate the μOR in GnRH neurons as a key player in the development of OIH. We have demonstrated that μOR activation alters CRE-mediated transcription, which may be a key mechanism in how morphine decreases GnRH secretion. In addition, we have shown that morphine treatment can alter GnRH neuron responsiveness and that μOR activation is responsible for this alteration. Finally, we have shown that chronic morphine treatment did not alter gene expression.

REFERENCES

1. Han B, Compton WM, Blanco C, Crane E, Lee J, Jones CM. Prescription Opioid Use, Misuse, and Use Disorders in U.S. Adults: 2015 National Survey on Drug Use and Health. Ann Intern Med. 2017;167(5):293-301.

2. Benyamin R, Trescot AM, Datta S, Buenaventura R, Adlaka R, Sehgal N, Glaser SE, Vallejo R. Opioid complications and side effects. Pain Physician. 2008;11(2 Suppl):S105-20.

3. Smith HS, Elliott JA. Opioid-induced androgen deficiency (OPIAD). Pain Physician. 2012;15(3 Suppl):ES145-56.

4. Abs R, Verhelst J, Maeyaert J, Van Buyten J-P, Opsomer F, Adriaensen H, Verlooy J, Van Havenbergh T, Smet M, Van Acker K. Endocrine Consequences of Long-Term Intrathecal Administration of Opioids. The Journal of Clinical Endocrinology & Metabolism. 2000;85(6):2215-22.

5. Kumar P, Kumar N, Thakur DS, Patidar A. Male hypogonadism: Symptoms and treatment. Journal of advanced pharmaceutical technology & research. 2010;1(3):297-301.

6. Colameco S, Coren JS. Opioid-induced endocrinopathy. J Am Osteopath Assoc. 2009;109(1):20-5.

7. Ranson, Ranson SW, Magoun HW. The hypothalamus. Ergebnisse der Physiologie, biologischen Chemie und experimentellen Pharmakologie. 1939;41(1):56-163.

8. Nakane PK. CLASSIFICATIONS OF ANTERIOR PITUITARY CELL TYPES WITH IMMUNOENZYME HISTOCHEMISTRY. Journal of Histochemistry & Cytochemistry. 1970;18(1):9-20.

9. Pinilla L, Aguilar E, Dieguez C, Millar RP, Tena-Sempere M. Kisspeptins and Reproduction: Physiological Roles and Regulatory Mechanisms. Physiological Reviews. 2012;92(3):1235-316.

10. Shaw ND, Histed SN, Srouji SS, Yang J, Lee H, Hall JE. Estrogen negative feedback on gonadotropin secretion: evidence for a direct pituitary effect in women. J Clin Endocrinol Metab. 2010;95(4):1955-61.

11. Kesner JS, Kaufman JM, Wilson RC, Kuroda G, Knobil E. The effect of morphine on the electrophysiological activity of the hypothalamic luteinizing hormone-releasing hormone pulse generator in the rhesus monkey. Neuroendocrinology. 1986;43(6):686-8.

12. Barkan AL, Duncan JA, Schiff M, Papavasiliou S, Garcia-Rodriguez A, Kelch RP, Marshall JC. Opioid and neurotransmitter regulation of pituitary gonadotropin-releasing hormone (GnRH) receptors in the ovariectomized estradiol-treated rat: role of altered GnRH secretion. Endocrinology. 1985;116(3):1003-10.

13. Al-Hasani R, Bruchas MR. Molecular mechanisms of opioid receptor-dependent signaling and behavior. Anesthesiology. 2011;115(6):1363-81.

14. Pfeiffer DG, Pfeiffer A, Shimohigashi Y, Merriam GR, Loriaux DL. Predominant involvement of mu-rather than delta- or kappa-opiate receptors in LH secretion. Peptides. 1983;4(5):647-9.

15. Panerai AE, Petraglia F, Sacerdote P, Genazzani AR. Mainly mu-opiate receptors are involved in luteinizing hormone and prolactin secretion. Endocrinology. 1985;117(3):1096-9.

16. Lagrange AH, Ronnekleiv OK, Kelly MJ. Estradiol-17 beta and mu-opioid peptides rapidly hyperpolarize GnRH neurons: a cellular mechanism of negative feedback? Endocrinology. 1995;136(5):2341-4.

17. Andrade A, Denome S, Jiang Y-Q, Marangoudakis S, Lipscombe D. Opioid inhibition of N-type Ca2+ channels and spinal analgesia couple to alternative splicing. Nature neuroscience. 2010;13(10):1249-56.

18. Karin M. Signal transduction and gene control. Current Opinion in Cell Biology. 1991;3(3):467-73.

19. Mellon PL, Windle JJ, Goldsmith PC, Padula CA, Roberts JL, Weiner RI. Immortalization of hypothalamic GnRH neurons by genetically targeted tumorigenesis. Neuron. 1990;5(1):1-10.

20. Kaufman DL, Keith DE, Jr., Anton B, Tian J, Magendzo K, Newman D, Tran TH, Lee DS, Wen C, Xia YR, Lusis AJ, Evans CJ. Characterization of the murine mu opioid receptor gene. J Biol Chem. 1995;270(26):15877-83.

21. Weibel R, Reiss D, Karchewski L, Gardon O, Matifas A, Filliol D, Becker JA, Wood JN, Kieffer BL, Gaveriaux-Ruff C. Mu opioid receptors on primary afferent nav1.8 neurons contribute to opiate-induced analgesia: insight from conditional knockout mice. PloS one. 2013;8(9):e74706-e.

22. Yoon H, Enquist LW, Dulac C. Olfactory inputs to hypothalamic neurons controlling reproduction and fertility. Cell. 2005;123(4):669-82.

23. Borrelli E, Montmayeur JP, Foulkes NS, Sassone-Corsi P. Signal transduction and gene control: the cAMP pathway. Critical reviews in oncogenesis. 1992;3(4):321-38.

24. Zhang X, Odom DT, Koo S-H, Conkright MD, Canettieri G, Best J, Chen H, Jenner R, Herbolsheimer E, Jacobsen E, Kadam S, Ecker JR, Emerson B, Hogenesch JB, Unterman T, Young RA, Montminy M. Genome-wide analysis of cAMP-response element binding protein occupancy, phosphorylation, and target gene activation in human tissues. Proceedings of the National Academy of Sciences of the United States of America. 2005;102(12):4459-64.

25. Kwakowsky A, Herbison AE, Ábrahám IM. The Role of cAMP Response Element-Binding Protein in Estrogen Negative Feedback Control of Gonadotropin-Releasing Hormone Neurons. The Journal of Neuroscience. 2012;32(33):11309-17.

26. Chen A, Laskar-Levy O, Ben-Aroya N, Koch Y. Transcriptional regulation of the human GnRH II gene is mediated by a putative cAMP response element. Endocrinology. 2001;142(8):3483-92.

27. Wetsel WC, Eraly SA, Whyte DB, Mellon PL. Regulation of gonadotropin-releasing hormone by protein kinase-A and -C in immortalized hypothalamic neurons. Endocrinology. 1993;132(6):2360-70.

28. Cheng Z, Garvin D, Paguio A, Stecha P, Wood K, Fan F. Luciferase Reporter Assay System for Deciphering GPCR Pathways. Current chemical genomics. 2010;4:84-91.

29. Nazian SJ, Landon CS, Muffly KE, Cameron DF. Opioid inhibition of adrenergic and dopaminergic but not serotonergic stimulation of luteinizing hormone releasing hormone release from immortalized hypothalamic neurons. Mol Cell Neurosci. 1994;5(6):642-8.

30. Pathan H, Williams J. Basic opioid pharmacology: an update. British journal of pain. 2012;6(1):11-6.

31. Czieselsky K, Prescott M, Porteous R, Campos P, Clarkson J, Steyn FJ, Campbell RE, Herbison AE. Pulse and Surge Profiles of Luteinizing Hormone Secretion in the Mouse. Endocrinology. 2016;157(12):4794-802.

32. Irwig MS, Fraley GS, Smith JT, Acohido BV, Popa SM, Cunningham MJ, Gottsch ML, Clifton DK, Steiner RA. Kisspeptin activation of gonadotropin releasing hormone neurons and regulation of KiSS-1 mRNA in the male rat. Neuroendocrinology. 2004;80(4):264-72.

33. Carretero J, Bodego P, Rodriguez RE, Rubio M, Blanco E, Burks DJ. Expression of the mu-opioid receptor in the anterior pituitary gland is influenced by age and sex. Neuropeptides. 2004;38(2-3):63-8.

34. Hoffmann HM, Larder R, Lee JS, Hu RJ, Trang C, Devries BM, Clark DD, Mellon PL. Differential CRE expression in Lhrh-Cre and Gnrh-Cre alleles and the impact on fertility in Otx2-flox mice. Neuroendocrinology. 2019.

35. De Maddalena C, Bellini M, Berra M, Meriggiola MC, Aloisi AM. Opioid-induced hypogonadism: why and how to treat it. Pain Physician. 2012;15(3 Suppl):Es111-8.

36. Fabian G, Bozo B, Szikszay M, Horvath G, Coscia CJ, Szucs M. Chronic morphine-induced changes in mu-opioid receptors and G proteins of different subcellular loci in rat brain. J Pharmacol Exp Ther. 2002;302(2):774-80.

37. Li S, Pelletier G. Opioid regulation of gonadotropin-releasing hormone gene expression in the male rat brain as studied by in situ hybridization. Neuroreport. 1993;4(3):331-3.

38. Zhang G, Lagrange AH, Ronnekleiv OK, Kelly MJ. Tolerance of hypothalamic beta-endorphin neurons to mu-opioid receptor activation after chronic morphine. J Pharmacol Exp Ther. 1996;277(1):551-8.

39. Khazali H, Mahmoudi F, Janahmadi M. Hypothalamic KiSS1/GPR54 Gene Expressions and Luteinizing Hormone Plasma Secretion in Morphine-treated Male Rats. International journal of fertility & sterility. 2018;12(3):223-8.

40. Yilmaz B, Konar V, Kutlu S, Sandal S, Canpolat S, Gezen MR, Kelestimur H. Influence of chronic morphine exposure on serum LH, FSH, testosterone levels, and body and testicular weights in the developing male rat. Arch Androl. 1999;43(3):189-96.

41. Miller WL. Steroidogenic acute regulatory protein (StAR), a novel mitochondrial cholesterol transporter. Biochim Biophys Acta. 2007;1771(6):663-76.

42. Lintern-Moore S, Supasri Y, Pavasuthipaisit K, Sobhon P. Acute and chronic morphine sulfate treatment alters ovarian development in prepuberal rats. Biol Reprod. 1979;21(2):379-83.

43. Belgorosky A, Guercio G, Pepe C, Saraco N, Rivarola MA. Genetic and clinical spectrum of aromatase deficiency in infancy, childhood and adolescence. Horm Res. 2009;72(6):321-30.

44. Aloisi AM, Ceccarelli I, Fiorenzani P, Maddalena M, Rossi A, Tomei V, Sorda G, Danielli B, Rovini M, Cappelli A, Anzini M, Giordano A. Aromatase and 5-alpha reductase gene expression: modulation by pain and morphine treatment in male rats. Mol Pain. 2010;6:69.